Dissertations, Theses, and Masters Projects   Theses, Dissertations, & Master Projects

1984

Acoustic radiation-induced static strain in single crystal silicon

Ka Kui Peter Li

College of William & Mary - Arts & Sciences

Recommended Citation

INFORMATION TO USERS

This reproduction was made from a copy of a document sent to us for microfilming. While the most advanced technology has been used to photograph and reproduce this document, the quality of the reproduction is heavily dependent upon the quality of the material submitted.

The following explanation of techniques is provided to help clarify markings or notations which may appear on this reproduction.

1. The sign or "target" for pages apparently lacking from the document photographed is "Missing Page(s)". If it was possible to obtain the missing page(s) or section, they are spliced into the film along with adjacent pages. This may have necessitated cutting through an image and duplicating adjacent pages to assure complete continuity.

2. When an image on the film is obliterated with a round black mark, it is an indication of either blurred copy because of movement during exposure, duplicate copy, or copyrighted materials that should not have been filmed. For blurred pages, a good image of the page can be found in the adjacent frame. If copyrighted materials were deleted, a target note will appear listing the pages in the adjacent frame.

3. When a map, drawing or chart, etc., is part of the material being photographed, a definite method of "sectioning" the material has been followed. It is customary to begin filming at the upper left hand corner of a large sheet and to continue from left to right in equal sections with small overlaps. If necessary, sectioning is continued again beginning below the first row and continuing on until complete.

4. For illustrations that cannot be satisfactorily reproduced by xerographic means, photographic prints can be purchased at additional cost and inserted into your xerographic copy. These prints are available upon request from the Dissertations Customer Services Department.

5. Some pages in any document may have indistinct print. In all cases the best available copy has been filmed.

8506858

Li, Ka Kui Peter

ACOUSTIC RADIATION-INDUCED STATIC STRAIN IN SINGLE CRYSTAL SILICON

The College of William and Mary in Virginia   Ph.D.   1984

University
Microfilms
International 300 N. Zeeb Road, Ann Arbor, MI 48106

PLEASE NOTE:

In all cases this material has been filmed in the best possible way from the available copy. Problems encountered with this document have been identified here with a check mark ___✓___.

1. Glossy photographs or pages ___✓___

2. Colored illustrations, paper or print _____

3. Photographs with dark background ___✓___

4. Illustrations are poor copy _____

5. Pages with black marks, not original copy _____

6. Print shows through as there is text on both sides of page _____

7. Indistinct, broken or small print on several pages ___✓___

8. Print exceeds margin requirements _____

9. Tightly bound copy with print lost in spine _____

10. Computer printout pages with indistinct print _____

11. Page(s) _____ lacking when material received, and not available from school or author.

12. Page(s) _____ seem to be missing in numbering only as text follows.

13. Two pages numbered _____. Text follows.

14. Curling and wrinkled pages _____

15. Other_____

ACOUSTIC RADIATION-INDUCED

STATIC STRAIN IN SINGLE CRYSTAL SILICON

———————————————

A dissertation

presented to

The faculty of the Department of Physics

The College of William and Mary in Virginia

In Partial Fulfillment

Of the Requirement for the Degree of

Doctor of Philosophy

———————————————

By

Ka Kui Peter Li

1984

APPROVAL SHEET

This dissertation is submitted in partial fulfillment
of the requirements for the degree of

Doctor of Philosophy

_____
author

Approved, November 1984

_____
J. H. Cantrell, Jr.   Chairman

_____
J. S. Heyman

_____
M. S. Conradi

_____
H. Krakauer

_____
W. T. Yost
NASA Langley Research Center

TABLE OF CONTENTS

iii

ACKNOWLEDGEMENTS

LIST OF TABLES

TABLE OF FIGURES

ABSTRACT

Quantitative verification of the existence of static acoustic displacements generated by acoustic waves propagating in single crystal samples of intrinsic silicon is presented. Measurements are made of the static dispalcements generated by 30 MHz acoustic compressional waves propagating along the [111], [110], and [100] crystalline directions. From these measurements the nonlinearity parameters are calculated and found to have the value 3.87 along the [111] direction, 4.23 along the [110] direction, and 2.13 along the [100] direction. These results are in agreement with values obtained independently from harmonic generation and pressure derivative measurements. Implications of the present work to the thermodynamics of single crystals are discussed.

ACOUSTIC RADIATION-INDUCED

STATIC STRAIN IN SINGLE CRYSTAL SILICON

INTRODUCTION

Nonlinearity must be accounted for in order to give a satisfactory description of the behavior of a solid. For example, thermal expansion,[1] the temperature dependence of acoustic velocity,[2] and optical rectification[3] are all nonlinear properties of a solid. To describe the nonlinear behavior of solids at the macroscopic level, the internal energy is assumed to be a function of the Lagrangian strains. The internal energy is usually expressed as a Taylor series expansion in the Lagrangain strains[4] and the constant coefficients of that expansion are identified as the Brugger elastic constants. If the internal energy is expanded in terms of the displacement gradients, the coefficients are refered to as the Huang elastic constants or propagation constants. The presence of terms higher than second order are attributed to the nonlinear behavior of solids.

It is well-known that when an initially sinusoidal finite amplitude wave propagates through a continuum second and higher harmonics, which grow linearly with the distance of propagation, are generated.[4-9] This phenonmenon is observed in liquids, gases and solids. The amplitude of the

second harmonic is directly proportional to the
nonlinearity parameter of the medium. In solids the
nonlinearity parameters are related to the generalized
Grüneisen parameters.[10,27]

Recent theoretical investigations of finite amplitude
acoustic waves in solids have predicted the existence
of a static displacement component generated by the
fundamental driving signal in addition to the harmonically
generated one.[11-13] However , there has been no direct
experimental evidence of this acoustic radiation-induced
static displacement until very recently.[14-16,38]

The objective of the present research is to provide
further quantitative verification of the existence of the
static acoustic displacement. We do this by measuring the
static displacement generated by an acoustic compressional
wave propagating in single crystal samples of intrinsic
silicon along the [111], [110], and [100] directions.
From these measurements the pure mode nonlinearity
parameters of silicon are calculated and compared to values
obtained by other methods.[4,17-18]

In section II the nonlinear acoustic wave equation is
solved to give the relationship among the acoustic static
displacement, the nonlinearity parameters, and the energy
density of the propagating wave. The analysis also provides
the expected shape of the static displacement signal. In
section III the experimental technique and procedure are

described and in section IV the experimental results are given. Section V discusses implications of the present work to the thermodynamics of single crystals. Calculations of generalized Grüneisen parameters with the assumption of the presence of static strain are given in appendix I.

II. THEORY

A. Fundamentals of the theory of finite deformation.

In the present investigation the wavelengths of the acoustic waves propagating in the solid samples are large compared to the inter-atomic spacing of the solid. The ratio of the inter-atomic spacing to the acoustic wavelength is of the order 10^{-4} to 1. Consequently the solid can be approximated as an elastic contiuum, and much information can be obtained from consideration of the thermoelastic properites of such a continuum.

The thermoelastic theory of solids[4,19-21] is based on the geometry of strain, and on three physical propositions: The first and second laws of thermodynamics, Newton's second law, and the rotational invariance of the state functions. According to this theory, the equilibrium states depend only on the configuration, denoted by x_i, and the entropy or the temperature per unit mass of the solids. Subsequently the state functions used in the thermoelastic theory are the Helmholtz free energy per unit mass or the internal energy per unit mass. Through the use of these state functions other thermodynamic relations, such as the stress-strain relation and the wave equation,

are derived. Traditionally, the state functions are
approximated by a series expansion in terms of their
independent variables. Thermodynamic relations are then
derived from these approximated state functions. We follow
this approach and obtain a nonlinear elastic wave equation
for solids. From this nonlinear wave equation, we show
that a static strain is generated by an acoustic wave
propagating in a solid.

In the following sections we present elements of the
thermoelastic theory pertinent to our study of solids.
First the finite deformation of solids is described by
introducing the concept of the Lagrangian strains. The
internal energy of solids is then written in terms of the
Lagrangian strains. Using the internal energy expression in
Lagrange's equation, the first order nonlinear wave equation
is derived. The equation describing the elastic displace-
ment due to the presence of an acoustic wave is then
obtained in the last section of this chapter.

1. The Lagrangian strains.

Consider an elastic continuum and let $a_i = (a_1, a_2, a_3)$
be the Cartesian coordinates of a material point in the
solid at time t_o in the unstrained state. Let
$x = (x_1, x_2, x_3)$ be the Cartesian coordinates of the same
material point at a later time t in the deformed state.
The displacement of a material point in the solid from its

initial unstrained state to its final deformed state is

$$u_i = x_i - a_i \qquad \cdot \qquad (1)$$

Under a homogeneous deformation the Cartesian coordinates in the deformed state is

$$x_i = a_i + u_{ij}a_j \qquad , \qquad (2)$$

where u_{ij} are the displacement gradients.

Using equation (1) and equation (2), the separation between the position of a material point in its unstrained and strained states becomes

$$r^2 - r_o^2 = x_i x_i - a_i a_i - 2n_{jk}a_j a_k \qquad , \qquad (3)$$

where

$$n_{ij} = \tfrac{1}{2}(u_{ij} + u_{ji} + u_{ki}u_{kj}) \qquad , \qquad (4)$$

are the Lagrangian strains.

The Lagrangian strains can also be expressed in terms of the Jacobian elements as

$$n_{ij} = \tfrac{1}{2}(J_{ki}J_{kj} - l_{ij}) \qquad , \qquad (5)$$

where

$$J_{ki} = \frac{\partial x_k}{\partial a_i} = \frac{\partial u_k}{\partial a_i} + I_{ki}$$

are the Jacobian elements, and

$$I_{ij} = \delta_{ij} \qquad\qquad (7)$$

are the usual Kronecker deltas.

Notice that under a finite rigid rotation of the material

$$J_{ki}J_{kj} = \delta_{ij} \qquad , \qquad\qquad (8)$$

and the Lagrangian strains are identically equal to zero. Thus the Lagrangian strains are invariant under a finite rigid rotation of the material. When the second order terms of the displacement gradients are neglected the Lagrangian strains reduce to

$$\epsilon_{ij} = \tfrac{1}{2}(u_{ij} + u_{ji}) \qquad , \qquad\qquad (9)$$

which are the infinitesimal strain measures in the linear elastic theory.

2. Internal energy of a strained solid.

Since the velocity of sound in a solid is several order of magnitude larger than the rate of heat

diffusion, the material deformed by a high frequency sound beam is, to a good approximation, done so adiabatically. The state function which characterizes this deformation process is then the internal energy.

The internal energy of a solid depends only on the relative positions of all the material particles and the entropy per unit mass. Recalling equation (3) we see that the relative positions of all the material particles in a solid are completely specified by the initial configuration a_i and the Lagrangian strains n_{ij} . Accordingly, the internal energy of a solid is

$$\Phi(a_i, n_{ij}, S) \qquad , \qquad (10)$$

Since the deformation from the initial configuration a_i to the final configuration x_i is usually small, it is convenient to expand the internal energy about the initial configuration a_i in terms of the Lagrangian strains n_{ij}. To configuration a_i in terms of the Lagrangian strains n_{ij}.

To third order of the Lagrangian strains,

$$\Phi = \Phi_0 + C_{ij}n_{ij} + \frac{1}{2} C_{ijkl}n_{ij}n_{kl} +$$

$$\frac{1}{6} C_{ijklmn}n_{ij}n_{kl}n_{mn} \qquad , \qquad (11)$$

where

$$c_{ij} = \frac{\partial \Phi}{\partial n_{ij}} \Big|_{n=0} \quad ,$$

$$c_{ijkl} = \frac{\partial^2 \Phi}{\partial n_{ij} \partial n_{kl}} \Big|_{n=0} \quad ,$$

and

$$c_{ijklmn} = \frac{\partial^3 \Phi}{\partial n_{ij} \partial n_{kj} \partial n_{mn}} \Big|_{n=0} \quad . \tag{12}$$

are the Brugger first, second, and third order elastic constants.[22]

Notice that since the Lagrangian strains are invariant under a finite rigid rotation of the material, the internal energy given in equation (11) also satisfies the same invariance property.

The thermodynamic tensions of the system are defined as[18-20]

$$\sigma_{ij} = \frac{\partial \Phi}{\partial n_{ij}} \quad . \tag{13}$$

Using equation (11) and equation (12), the thermodynamic tensions of a solid are expressed in terms of the Lagrangian strains as

$$\sigma_{ij} = C_{ij} + C_{ijkl}\eta_{kl} + \frac{1}{2}C_{ijklmn}\eta_{kl}\eta_{mn} \quad . \qquad (14)$$

Note that in an initially stress free configuration the Lagrangian strains in equation (14) vanish, and

$$C_{ij} = 0 \quad . \qquad (15)$$

We may thus write the internal energy of a solid with no initial stress as

$$\Phi = \frac{1}{2}C_{ijkl}\eta_{ij}\eta_{kl} + \frac{1}{6}C_{ijklmn}\eta_{ij}\eta_{kl}\eta_{mn} \quad . \qquad (16)$$

Since there are four indices for the second order elastic constants and six indices for the third order elastic constants, there are a total of 81 second order elastic constants and 729 third order elastic constants. Fortunately, the crystalline symmetry of solids reduces the number of independent elastic constants.[18] For a cubic crystal, such as silicon, there are only three second order elastic constants and six third order elastic constants.

From equation (4), we see that the Lagrangian strains are symmetric. Therefore only six of the nine strain elements are independent of each other. Using this symmetry property, we can simplify equation (16) by

contracting the subscript notation according to the Voigt (1928) convention, in which one index replaces a pair of indices according to the following scheme:

$$11 \longrightarrow 1 \quad 22 \longrightarrow 2 \quad 33 \longrightarrow 3 \quad 23 \longrightarrow 4 \quad 13 \longrightarrow 5 \quad 12 \longrightarrow 6$$

Using the Voigt notation the complete set of second and third order Brugger elastic constants for cubic crystals reduces to

$$c_{11} , c_{12} , c_{13} ,$$

and

$$c_{111} , c_{112} , c_{113} , c_{144} , c_{166} , c_{456} .$$

From this scheme, the second and third terms of the internal energy can be written in the following forms:

$$\frac{1}{2} c_{ijkl} n_{ij} n_{kl} = \frac{1}{2} c_{11} (n_{11}^2 + n_{22}^2 + n_{33}^2) +$$

$$c_{12} (n_{11} n_{22} + n_{22} n_{33} + n_{33} n_{11}) +$$

$$c_{44} (n_{12}^2 + n_{21}^2 + n_{23}^2 + n_{32}^2 + n_{31}^2 + n_{13}^2)$$

and

$$\frac{1}{6} C_{ijklmn} n_{ij} n_{kl} n_{mn} =$$

$$\frac{1}{6} C_{111}(n_{11}^3 + n_{22}^3 + n_{33}^3) +$$

$$\frac{1}{2} C_{112}[n_{11}^2(n_{22} + n_{33}) + n_{22}^2(n_{33} + n_{11}) + n_{33}^2(n_{11} + n_{22})]$$

$$+ C_{123}(n_{11}n_{22}n_{33}) + C_{456}[(n_{12} + n_{21})(n_{23} + n_{32})(n_{31} +$$

$$n_{31})] + C_{144}[n_{11}(n_{23}^2 + n_{32}^2) + n_{22}(n_{31}^2 + n_{13}^2) +$$

$$n_{33}(n_{12}^2 + n_{21}^2)] + C_{166}[(n_{12}^2 + n_{21}^2)(n_{11} + n_{22}) +$$

$$(n_{23}^2 + n_{32}^2)(n_{22} + n_{33}) + (n_{31}^2 + n_{13}^2)(n_{33} + n_{11})] \qquad (17)$$

Since it is the displacements of the material points that one usually measures in an experiment, it is convenient to write the internal energy in terms of the displacement gradients. To third order[25]

$$\Phi = \frac{1}{2} A_{ijkl} u_{ij} u_{kl} + \frac{1}{6} A_{ijklmn} u_{ij} u_{kl} u_{mn} \qquad , \qquad (18)$$

where

$$A_{ijkl} = \frac{\partial^2 \Phi}{\partial u_{ij} \partial u_{kl}} \qquad . \tag{19}$$

and

$$A_{ijklmn} = \frac{\partial^3 \Phi}{\partial u_{ij} \partial u_{kl} \partial u_{mn}}$$

are defined as the second and third order Huang elastic constants or the propagation constants. The relation-ships between the Huang and Brugger elastic constants are obtained readily by eliminating the Lagrangian strains in equation (16) in favor of the displacement gradients. Since all the u_{ij} are independent, the coefficients in equation (16) and equation (18) must be equal

$$A_{ijkl} = C_{ijkl} \qquad , \tag{20}$$

$$A_{ijklmn} = C_{jlmn}\delta_{ik} + C_{ijnl}\delta_{km} + C_{jknm}\delta_{im} + C_{ijklmn} \quad .$$

It is necessary to point out that in obtaining equation (20) we have identified $\Phi(u_{ij})$ with $\Phi(n_{ij})$. Therefore, the internal energy given in equation (18) is rotationally invariant.

B. The equations of motion.

Under the conditions for which the attenuation and dispersion are negligible the displacement field of an acoustic wave in a continuous medium can be derived from Lagrange's equation [26]

$$\frac{\partial}{\partial t}\frac{\partial L}{\partial \dot{x}_i} + \frac{\partial}{\partial a_k}\frac{\partial L}{\partial\left(\frac{\partial x_i}{\partial a_k}\right)} - \frac{\partial L}{\partial x_i} = 0 \tag{21}$$

where the Lagrangian of a solid is

$$L = \frac{1}{2}\rho_0 \dot{u}_i \dot{u}_i - \Phi \tag{22}$$

In equation (22) $\dot{u}_i$ is the particle velocity and ρ_0 is the unstrained mass density of the solid. Substituting equation (22) into Lagrange's equation, we get

$$\ddot{u}_i = \frac{\partial}{\partial a_j}\frac{\partial \Phi}{\partial u_{ij}} \tag{23}$$

Using equation (18) in equation (23) and collecting the displacement gradient terms up to second order we obtain

$$\rho_0 \ddot{u}_i = \left(A_{ijkl} + A_{ijklmn}\frac{\partial u_m}{\partial a_n} \right) \frac{\partial^2 u_k}{\partial a_j \partial a_l} \tag{24}$$

Since we are considering plane waves propagating in a given direction, we can simplify equation (24) by introducing a rotational transformation R

$$\bar{a}_j = R_{jk} a_k \qquad (25)$$

defined such that the a_1-axis is oriented along the wave propagation direction a_1.

Since the elastic energy is a scalar, we may write for a finite rigid rotation of the material that

$$\Phi(n) = \Phi(\bar{n}) = \Phi(R_{j1} R_{tk} \bar{n}_{jt}) \qquad , \qquad (26)$$

or

$$\Phi = \frac{1}{2} \bar{C}_{ijkt} \bar{n}_{ij} \bar{n}_{kt} + \frac{1}{6} \bar{C}_{ijktmn} \bar{n}_{ij} \bar{n}_{kt} \bar{n}_{mn} \qquad . \qquad (27)$$

In terms of the Huang elastic constants we obtain

$$\Phi = \frac{1}{2} \bar{A}_{ijkt} \bar{u}_{ij} \bar{u}_{kt} + \frac{1}{6} \bar{A}_{ijktmn} \bar{u}_{ij} \bar{u}_{kt} \bar{u}_{mn} \qquad . \qquad (28)$$

The elastic constants in the initial coordinate frame are related to those in the rotated coordinate frame by the following transformations:

$$\bar{C}_{ijkt} = R_{ip}R_{jq}R_{kr}R_{ts}C_{pqrs} \qquad ,$$

and

$$\bar{C}_{ijktmn} = R_{ip}R_{jq}R_{kr}R_{ts}R_{mu}R_{nv}C_{pqrsuv} \quad . \tag{29}$$

The relationships between the Huang elastic constants and the Brugger elastic constants in the rotated coordinate are the same as those given in equation (20) except A_{ijkt} is replaced by $\bar{A}_{ijkt}$, C_{ijkt} by $\bar{C}_{ijkt}$, etc.

The wave equation in the rotated coordinate frame is

$$\rho_0 \ddot{\bar{u}}_i = (\bar{A}_{ijkt} + \bar{A}_{ijktmn}\frac{\partial \bar{u}_m}{\partial \bar{a}_n}) \frac{\partial^2 \bar{u}_k}{\partial \bar{a}_j \partial \bar{a}_t} \quad . \tag{30}$$

For a plane wave with propagation direction parallel to the $\bar{a}_1$- axis

$$\rho_0 \ddot{\bar{u}}_i = (\bar{A}_{i1k1} + \bar{A}_{i1k1m1}\frac{\partial \bar{u}_m}{\partial \bar{a}_1}) \frac{\partial^2 \bar{u}_k}{\partial \bar{a}_1^2} \quad . \tag{31}$$

To simplify equation (31) we define the matrices[27,28]

$$\bar{A}_{i1k1} = D_{ik}$$

and

$$\bar{A}_{11k1m1} = D_{1km} \qquad . \qquad (32)$$

Using these definitions the wave equation simplifies to

$$\rho_o \ddot{\bar{u}}_i = (D_{ik} + D_{1km} \frac{\partial \bar{u}_k}{\partial \bar{a}_1}) \frac{\partial^2 \bar{u}_k}{\partial \bar{a}_1^2} \qquad (33)$$

Since D_{ik} is a symmetric matrix, an orthogonal transformation S is guaranteed to exist such that $S_{kq} D_{qr} S_{r1}$ is diagonalized. Defining such a transformation by

$$\bar{u}_k = S_{kq} P_q \qquad , \qquad (34)$$

and applying the transformation to equation (33) we get

$$\rho_o S_{pi}^{-1} S_{iq} \frac{\partial^2 P_q}{\partial t^2} = S_{pi}^{-1} D_{ik} S_{kq} \frac{\partial^2 P_q}{\partial \bar{a}_1^2} \qquad ,$$

$$S_{pi}^{-1} D_{ikm} S_{kr} S_{ms} \frac{\partial P_r}{\partial \bar{a}_1} \frac{\partial^2 P_s}{\partial \bar{a}_1^2} \qquad , \qquad (35)$$

where the superscript -1 denoted the inverse transformation. Since S is orthogonal,

$$S_{pi}D_{ik}S_{kq} = \mu_p \delta_{pq} \qquad , \qquad (36)$$

and the wave equation (35) becomes

$$\rho_0 \ddot{P}_q = \mu_q \frac{\partial^2 P_q}{\partial \bar{a}_1^2} + \nu_{qrs} \frac{\partial P_r}{\partial \bar{a}_1} \frac{\partial^2 P_s}{\partial \bar{a}_1^2} \qquad , \qquad (37)$$

where

$$\mu_q = S_{qi}^{-1}D_{ik}S_{kq} \qquad (38)$$

are the eignvalues for the matrix D_{ik} and

$$\nu_{qrs} = S_{qi}^{-1}D_{ikm}S_{kr}S_{ms} \qquad (39)$$

are known linear combinations of the second and third
order elastic constants. Equation (37) is exact
through the lowest order nonlinear terms.   A
straightforward perturbation calculation shows that the
mutual resonant terms (i.e. those such that the indices
r=q=s) are several order of magnitude larger than the
remaining nonresonant terms. Keeping only the mutual
resonant terms, we find that the equation of motion
for a plane wave with propagation direction along the
$\bar{a}_1$- axis becomes

$$\rho_0 \frac{\partial^2 P_j}{\partial t^2} = \mu_j \frac{\partial^2 P_j}{\partial \bar{a}_1^2} + \nu_{jjj} \frac{\partial P_j}{\partial \bar{a}_1} \frac{\partial^2 P_j}{\partial \bar{a}_1^2} \qquad . \qquad (40)$$

In equation (40) the repeated j's are not summed. The index j specifies the polarization direction of an acoustic wave.

Now let us rewrite the nonlinear wave equation in the form

$$\frac{\partial^2 P_j}{\partial t^2} = \frac{\mu_j}{\rho_0} \left(1 + \frac{\nu_{jjj}}{\mu_j} \frac{\partial P_j}{\partial \bar{a}_1} \right) \frac{\partial^2 P_j}{\partial \bar{a}_1^2} \qquad . \qquad (41)$$

and define the acoustic nonlinearity parameters for solids by [10]

$$\beta_j = \frac{\nu_{jjj}}{\mu_j} \qquad , \qquad (42)$$

and the infinitesmial amplitude wave velocity for solids by

$$c_j = \left(\frac{\mu_j}{\rho_0} \right)^{\frac{1}{2}} \qquad . \qquad (43)$$

With these definitions the nonlinear wave equation simplifies to

$$\frac{\partial^2 P_j}{\partial t^2} = c_j^2 \left(1 - \beta_j \frac{\partial P_j}{\partial \bar{a}_1} \right) \frac{\partial^2 P_j}{\partial \bar{a}_1^2} \qquad . \qquad (44)$$

The nonlinearity parameters for an acoustic wave propagating along the [111], [110], and [100] directions of a cubic crystal are given in table (1). It is important to point out that when $\beta_j = 0$ the nonlinear wave equation reduces to the linear wave equation

$$\frac{\partial^2 P_j}{\partial t^2} = c_j^2 \frac{\partial^2 P_j}{\partial \bar{a}_1^2} \qquad (45)$$

Writing equation (45) in the form

$$\left(\frac{\partial}{\partial t} - c_j \frac{\partial}{\partial \bar{a}_1} \right) \left(\frac{\partial}{\partial t} + c_j \frac{\partial}{\partial \bar{a}_1} \right) P_j = 0 \qquad , \qquad (46)$$

we readily see that for an acoustic wave propagating in the positive coordinate direction an appropriate form of the linear wave equation is

$$\frac{\partial P_j}{\partial t} = -c_j \frac{\partial P_j}{\partial \bar{a}_1} \qquad , \qquad (47)$$

in which the particle velocity $\frac{\partial P_j}{\partial t}$, the displacement gradients $\frac{\partial P_j}{\partial \bar{a}_1}$ are directly proportional to each other.

NONLINEARITY PARAMETERS FOR [100], [110], AND [111] DIRECTIONS.

$$\left(\beta_j = -\frac{3K_2 + K_3}{K_2}\right).$$

DIRECTION	K_2	K_3
[100]	C_{11}	C_{111}
[110]	$\dfrac{C_{11} + C_{12} + 2C_{44}}{2}$	$\dfrac{C_{111} + 3C_{112} + 12C_{166}}{4}$
[111]	$\dfrac{C_{11} + 2C_{12} + 4C_{44}}{3}$	$\dfrac{C_{111} + 6C_{112} + 12C_{144} + 24C_{166} + 2C_{123} + 16C_{456}}{9}$

Table (1)

In order to obtain a corresponding relationship between the particle velocity and the displacement gradient for the case of nonzero β_j , we assume that the particle velocity can be expressed as a function of the displacement gradients in the form [37]

$$\frac{\partial P_j}{\partial t} = f\left(\frac{\partial P_j}{\partial \bar{a}_1}\right) \quad , \tag{48}$$

where f is some continuous differentiable function of $\partial P_j/\partial\bar{a}_1$. Differentiating equation (48) with respect to time t gives

$$\frac{\partial^2 P_j}{\partial t^2} = f' \frac{\partial^2 P_j}{\partial\bar{a}_1\partial t} \quad , \tag{49a}$$

while differentiating with respect to the Lagrangian corrdinate $\bar{a}_1$ gives

$$\frac{\partial^2 P_j}{\partial t\partial\bar{a}_1} = f' \frac{\partial^2 P_j}{\partial\bar{a}_1^2} \quad . \tag{49b}$$

Here f' denotes differentiation of f with respect to $\partial P_j/\partial\bar{a}_1$. Substituting equation (49b) into equation (49a) we get

$$\frac{\partial^2 P_j}{\partial t^2} = (f')^2 \frac{\partial^2 P_j}{\partial \bar{a}_1^2} \qquad . \qquad (50)$$

comparing equation (50) with the nonlinear wave equation (44) we obtain the identity:

$$f' = c_j \left(1 - \beta_j \frac{\partial P_j}{\partial \bar{a}_1} \right)^{\frac{1}{2}} \qquad . \qquad (51)$$

Integrating equation (51) with respect to $\partial P_j / \partial \bar{a}_j$ and recalling that $f' = \partial P_j / \partial t$, we obtain the relationship between the particle velocity and the displacement gradient for a nonlinear wave equation in the form

$$\frac{\partial P_j}{\partial t} = \frac{2}{3} \frac{c_j}{\mu_j} \left(1 - \beta_j \frac{P_j}{\bar{a}_1} \right)^{\frac{3}{2}} - \frac{3}{2} \frac{c_j}{\mu_j} \qquad . \qquad (52)$$

The integration constant in equation (52) is obtained for the condition that the particle velocity is zero when the displacement gradients is zero. Solving equation (52) for $\partial P_j / \partial \bar{a}_1$ and expanding the result to the second power of the particle velocity we obtain

$$\frac{\partial P_j}{\partial \bar{a}_1} = - \frac{1}{c_j} \frac{\partial P_j}{\partial t} + \frac{\beta_j}{4c_j} \left(\frac{\partial P_j}{\partial t} \right)^2 \qquad . \qquad (53)$$

C. Static displacement generated by an acoustic wave propagating in a solid.

The particle velocity solution of the nonlinear wave equation (44) subject to the boundary condition that

$$\frac{\partial P_j}{\partial t} = \left(\frac{\partial P_j}{\partial t}\right)_o \sin\omega t \tag{54}$$

at $a_1 = 0$ has been solved by Fubini[19]. His solution is written in the form

$$\frac{\partial P_j}{\partial t} = \left(\frac{\partial P_j}{\partial t}\right)_o \sin(\omega t - k\bar{a}_1) +$$

$$\frac{1}{4}\left(\frac{\partial P_j}{\partial t}\right)_o^2 \frac{k}{c_j} \beta_j \bar{a}_1 \sin 2(\omega t - k\bar{a}_1) \quad . \tag{55}$$

Let Q be a quantity which is a function of time and material coordinate a_1 . We define the time-average of Q by

$$\langle Q \rangle = \lim_{t \to} \frac{1}{t}\int_o^t Q(t',\bar{a}_1)dt' \quad . \tag{56}$$

Using the Fubini solution in equation (53) and time averaging the results, we find

$$\left\langle \frac{\partial P_j}{\partial a_j}\right\rangle = -\frac{1}{8}\beta_j k^2 (P_j)_o^2 \quad . \tag{57}$$

Equation (57) can also be written in terms of the energy density of the acoustic wave in the form

$$\left\langle \frac{\partial P_j}{\partial a_1} \right\rangle = -\frac{1}{4} \frac{\beta_j}{\mu_j} \langle E \rangle \qquad , \qquad (58)$$

where

$$\langle E \rangle = \frac{1}{2} \mu_j (P_j)_0^2 \qquad . \qquad (59)$$

For a solid with nonzero β_j equations (57) and (58) predict the existence of an acoustically-induced static strain accompanying the propagation of an acoustic wave in a solid.

Equations (57) and (58) are obtained for a continuous wave propagating in a semi-infinite half space. In the present investigation, however, a gated acoustic pulse or toneburst is propagted through a sample of finite size. Let us consider the theoretical implication of such an experimental situation. Consider an acoustic toneburst of length L, amplitude P_j, and frequently f as shown in the top panel of figure (1). The energy density of the acoustic signal is nonzero only within the spatial extent of the toneburst. Hence the acoustically-induced static strain is defined only within that region of space as shown in panel (b) of the figure. If the measurement technique used in

(a)

ULTRASONIC
TONE-BURST.

$(P_j)_o$

(b)

STATIC
STRAIN PULSE.

$< \partial P_j / \partial a >$

(c)

STATIC
DISPLACEMENT
PULSE.

$1/8 \, k^2 \beta_j (P_j)_o^2 \, L$

$\vdash L = C_j \Delta t \dashv$

DIRECTION OF PROPAGATION
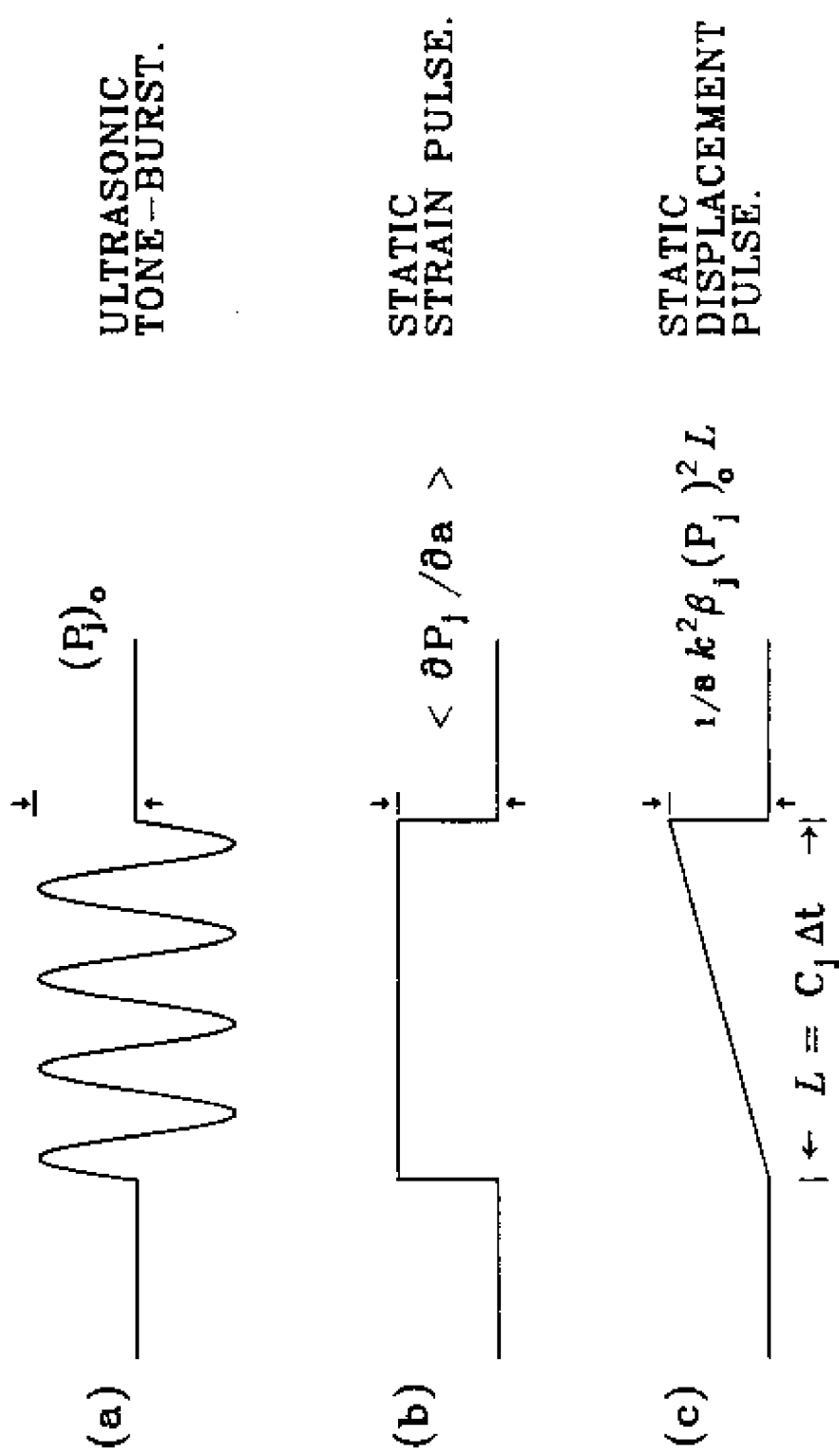
figure (1)

measuring the acoustic signal is sensitive to the static
strain amplitude, the signal detected will be a square
pulse as shown. In our experiment the detector used is
sensitive only to the acoustic displacement amplitude.
Integrating along the length of the acoustic pulse gives

$$P_j = \int_0^{\bar{a}_1} \frac{1}{8} k^2 \beta_j (P_j)_o^2 \, d\bar{a}_j$$

$$= \frac{1}{8} k^2 \beta_j (P_j)_o^2 \, \bar{a}_1 \qquad . \qquad (60)$$

From this equation we see that the static displacement
amplitude is a right-angled triangular pulse. The slope
of this static acoustic displacement pulse is

$$\frac{\Delta P_j}{c_j \Delta t} = \frac{1}{8} \frac{k^2}{c_j} \beta_j (P_j)_o^2 \qquad . \qquad (61)$$

Equation (61) gives the displacement amplitude of the
static displacement accompanying the propagating tone-
burst inside the solid. When this displacement pulse
reaches the free end of the solid its amplitude doubles
to

$$P_j = \frac{1}{4} k^2 \beta_j (P_j)_o^2 \, \bar{a}_1 \qquad (62)$$

in order to satisfy the stress free surface boundary

condition.

We see from equation (62) that the static displacement is directly proportional to the nonlinearity parameter. A positive nonlinearity parameter produces a positive static displacement signal, while a negative nonlinearity parameter produces a negative static displacement signal. Most cubic and isotropic materials have positive nonlinearity parameters.[5,6] However, fused silica has a negative nonlinearity parameter.[7,8] Consequently for most solids the presence of an acoustic wave produces a static expansion while for fused silica the presence of an acoustic wave produces a static contraction.

III. APPARATUS, PROCEDURES, AND SAMPLES.

A. Experimental considerations.

The primary objective of the present investigation is to provide quantitative confirmation of the existence of the acoustically induced static displacements by accurately determining the value of the nonlinearity parameters appearing in equation (61) for each sample under study. In order to make such quantitative measurements both the slope of the acoustic static displacement and the amplitude of the fundamental must be determined absolutely. We note from equation (61) that the static displacement is proportional to the square of the frequency of the fundamental wave. Hence, a high frequency fundamental signal is preferred for better signal-to-noise ratio. However, equation (61) is obtained under the assumptions that attenuation and dispersion can be neglected. Thus, to assure the success of the experiment, careful consideration in selecting the frequency range for the measurement is necessary. the most important considerations are those of phase cancellation effects, attenuation, and diffraction.

30

1. Phase cancellation effect.

For simplicity let us consider a plane wave impinging on the lower surface of a specimen as shown in figure (2). If the angle of incidence of the acoustic wave is small, the phase angle of the wave at position r relative to point a can be approximated by

$$p = \frac{r \sin(\theta)}{c} \quad , \quad (63)$$

where ω is the frequency, and c is the velocity of the acoustic signal. Thus, we can express the spatially averaged amplitude of an acoustic signal impinging at the lower surface at time t_0 in the form

$$\bar{A} = \frac{1}{r} \int_0^{r} A_0 \sin(\omega t + p) \, dr \quad . \quad (64)$$

Using a trigonometric identity we can write

$$\bar{A} = A_0 \sin(\omega t) \frac{1}{\delta} \int_0^{\delta} \cos(p) \, dr +$$

$$A_0 \cos(\omega t) \frac{1}{\delta} \int_0^{\delta} \sin(p) \, dr \quad . \quad (65)$$

Carrying out the integration we obtain

$$\frac{\bar{A}}{A_o} = \frac{\sin\left(\frac{\delta\pi}{\lambda}\sin\theta\right)}{\frac{\delta\pi}{\lambda}\sin\theta}\,\sin\left(\omega t + \frac{\delta\pi}{\lambda}\sin\theta\right) , \tag{66}$$

where

$$\lambda = \frac{\omega}{2\pi c} , \tag{67}$$

when is small

$$\frac{\bar{A}}{A_o} \sim (1-\alpha)\sin(\omega t + \phi) , \tag{68}$$

where

$$\alpha \sim \frac{1}{3}\left(\frac{\pi\delta}{\lambda}\right)^2 , \tag{69}$$

and

$$\phi = \arctan\left(\frac{\pi\delta}{\lambda}\right) . \tag{70}$$

From equation (68) we see that the nonparallelism of the sample surfaces introduces an apparent attenuation to the amplitude and a change in the phase angle of the acoustic signal. An acoustic wave having a frequency in the range of a few MHz will have a wavelength of about 10^{-4} m for most solids. Thus to assure that the apparent
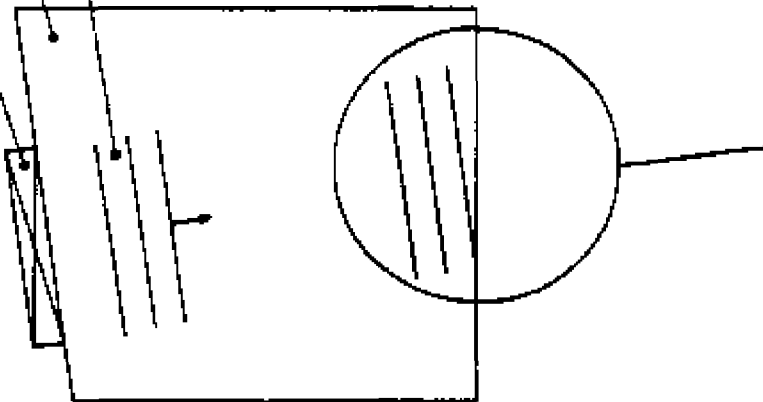
x = The acoustic path difference between points a and b of the wave front to the bottom surface of the specimen

δ = The width of the surface which senses the acoustic signal

ε = The hight of the right-angled triangle

θ = Angle of incidence

figure (2)

33
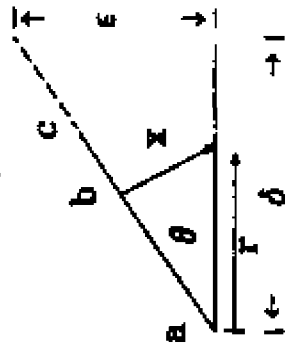
attenuation α of the acoustic signal due to
nonparallelism of the sample surfaces is within one
percent, ϵ must be of the order of a few microns. It is
not difficult to achieve parallelism with such tolerances
by careful polishing. It does, however, become
increasingly difficult to polish the surfaces to the
tolerances required when the frequency of the acoustic
signal increases to about 100 MHz.

It is important to point out that the nonparallelism
of the sample surfaces does not introduce a static
component into the detected signal. Further the
frequency of the acoustic signal remains invariant
under such condition.

2. Attenuation consideration.

Since acoustic attenuation is neglected in obtaining
equation(61), we must choose to work in a frequency
range where acoustic attenuation is not significant.
In general acoustic attenuation increases with increasing
frequency, and in the MHz frequency range it is
proportional to the square of the frequency. Thus to
ignore the effect of attenuation we must work in the
low MHz frequency range.

3. Diffraction consideration.

One other experimental consideration which must be addressed is the diffraction of the acoustic beam as it propagates away from the transducer. Since the transducer used in the experiment is of finite size, the acoustic wave radiating from the transducer will spread out subtending an angle[23]

$$= \sin^{-1}(1.22 \frac{\lambda}{a}) \quad , \qquad (71)$$

where a is the diameter of the transducer. To minimize the diffraction angle a transducer with a large diameter must be used in the measurement. We have chosen a $\frac{1}{2}$ inch 30 MHz transducer for the experiments. The diffraction angle is calculated to be about one degree. The apparent attenuation due to diffraction is therefore unimportant in the present experiment and no diffraction corrections are used.

Figure 3.

36
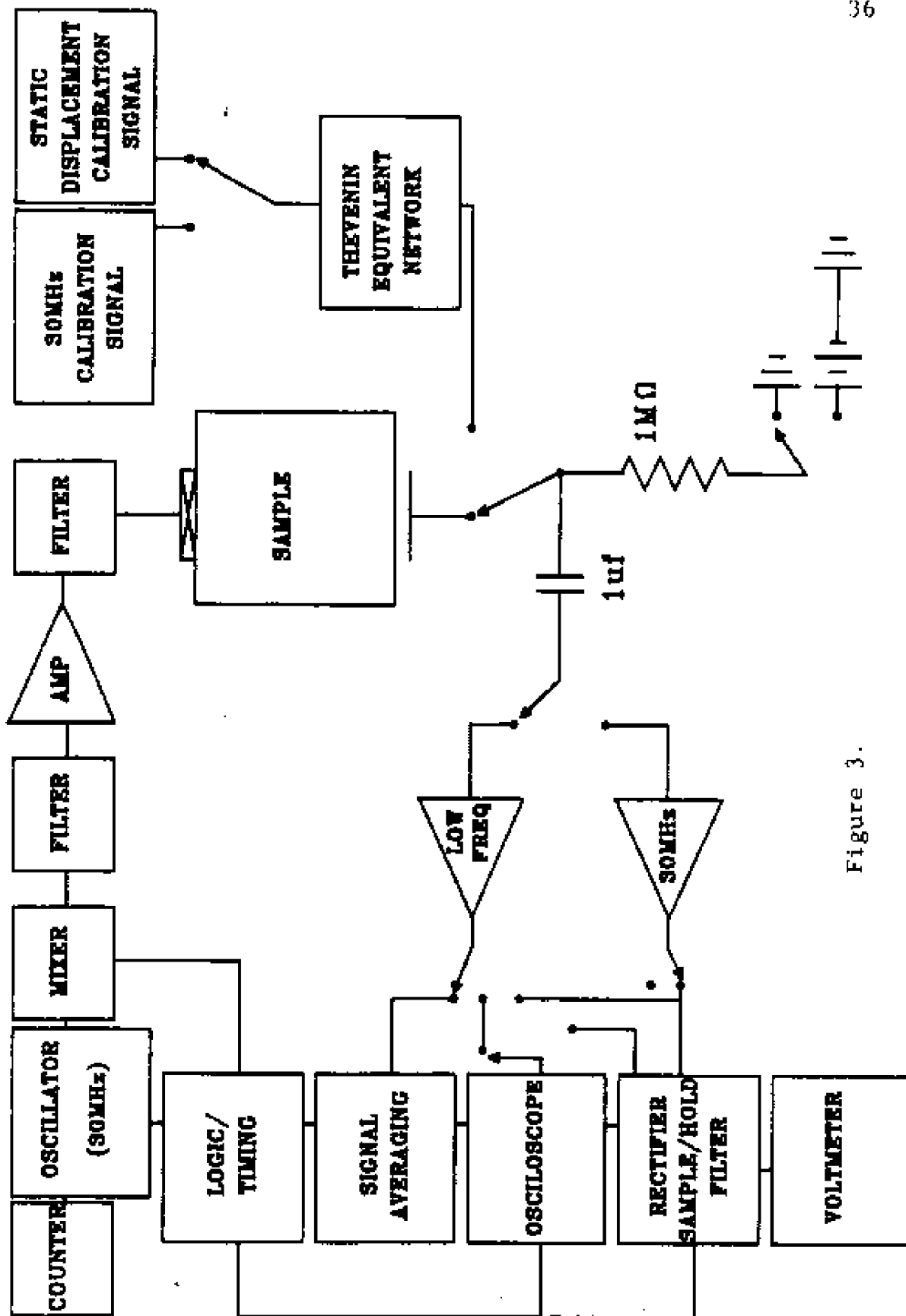
B. Apparatus and measurement technique.

A block diagram of the experimental setup is shown in figure (3). A gated 30 MHz ultrasonic signal is obtained by mixing a 30 MHz continuous RF signal generated by a Hewlett-Packard 606B signal generator with a square pulse generated by a logic/timing unit. The resulting RF pulse is then filtered by an 8 MHz passive high pass filter to remove any leakage of the gating pulse throught the mixer. The amplified RF signal is fed to a 13 MHz passive high pass filter, and the filtered signal is then used to drive a 30 MHz narrow band Lithium Niobate transducer bonded to one end of the sample.

When the transducer is excited by the gated 30 MHz electrical signal, it launchs a 30 MHz gated acoustic wave into the sample. The ultrasonic wave is detected at the opposite end of the sample by a capacitive transducer. The signal from the capacitive transducer is then fed either to the 30 MHz preamplifier for fundamental displacement amplitude measurements, or to the low frequency preamplifier for static acoustic displacement measurements.

Since the fundamental signal is a gated RF signal and the static acoustic signal is a short duration pulse, the band width of the amplifier must be wide enough to reproduce short duration acoutic tonebursts.

In our experiment a broad band ENI model 3001 RF amplifier with a 40 dB gain is used to amplify the fundamental acoustic signals, and a Princeton Applied Reasearch model 113 low-frequency (3-300 KHz) preamplifier is used to amplify the static acoustic displacement signals.

1.   Ultrasonic transmission-receiving assembly .

The amplitude of the fundamental acoustic wave generated by a lithium niobate transducer is typically of the order of a few Angstroms. The nonlinearity parameters calculated from the second and third order elastic constants[23] typically range from a value of 2 to 20. According to equation (60), then, the static acoustic displacements are of the order 10^{-2} Angstroms. We see that our receiving transducer not only must have a wide frequency bandwidth but also must have sufficient sensitivity to detect very small amplitude signals. For this reason a capacitive transducer was constructed to receive the acoustic signals for these experiments.

Ground ring

Teflon

Electrode

Transducer

Electrode

Ground ring

Glass plate

Housing

Sample
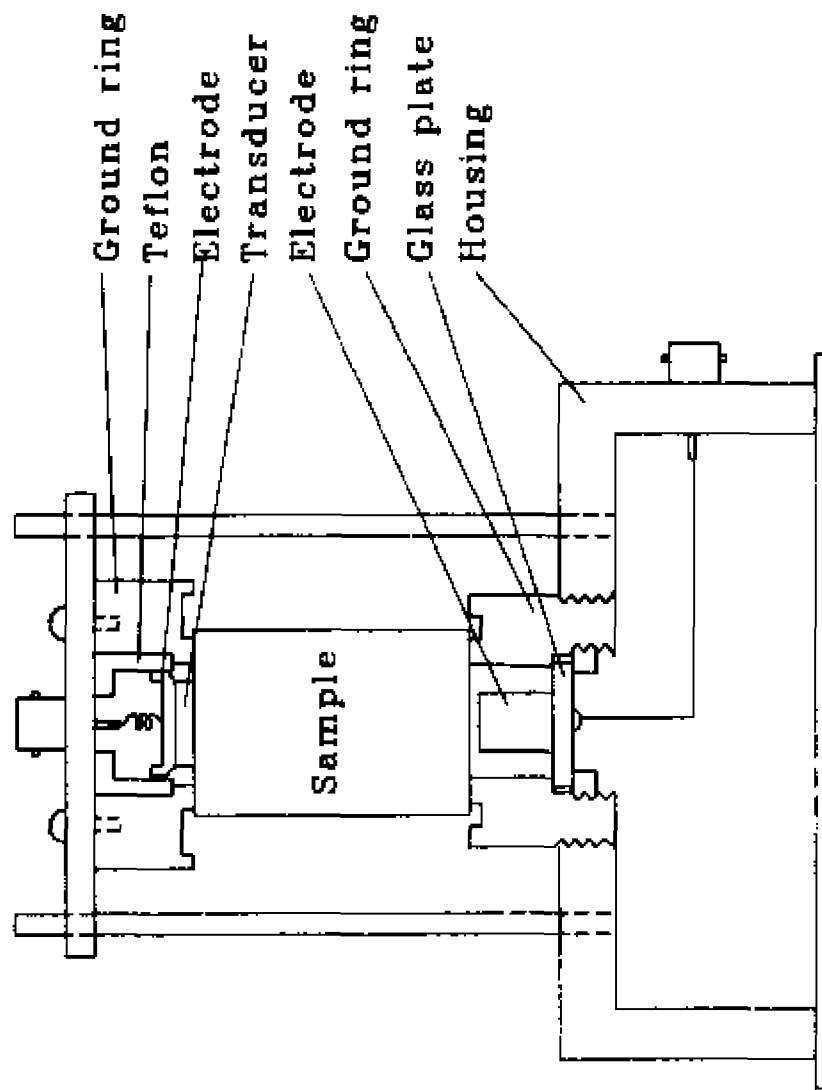
figure (4)

a. Mechanical parts of the transmission-receiving assembly.

A diagram of the mechanical parts of the transmission and receiving assembly is shown in figure (4) The assembly consists of an ultrasonic wave transmission unit and a signal receiving unit.

The sample rests on the outer ground ring of the receiving unit so that one end surface becomes the top plate of a parallel plate capacitor. The detecting electrode at the center of the receiver forms the other surface of the parallel plate capacitor. The detecting electrode is isolated from the ground ring by a glass plate. A bias voltage, about 50 volt, is applied across the parallel plate to create an electric field in the gap spacing. Therefore, when the acoustic signal impinges on the sample surface the gap spacing varies and converts the acoustic vibrations into an electrical signal.

A 30 MHz compressional lithium niobate transducer is bonded at the other end of the sample by a thin layer of phenyl salicylate. The ground ring of this transmission unit rests on the outer surface of the sample and a copper electrode in the center of the transmission unit provides electrical contact with one end of the lithium niobate transducer. Figure (5) shows the detector assembly before the sample is mounted ,

Figure 5. - The detector assembly before the
sample is mounted.
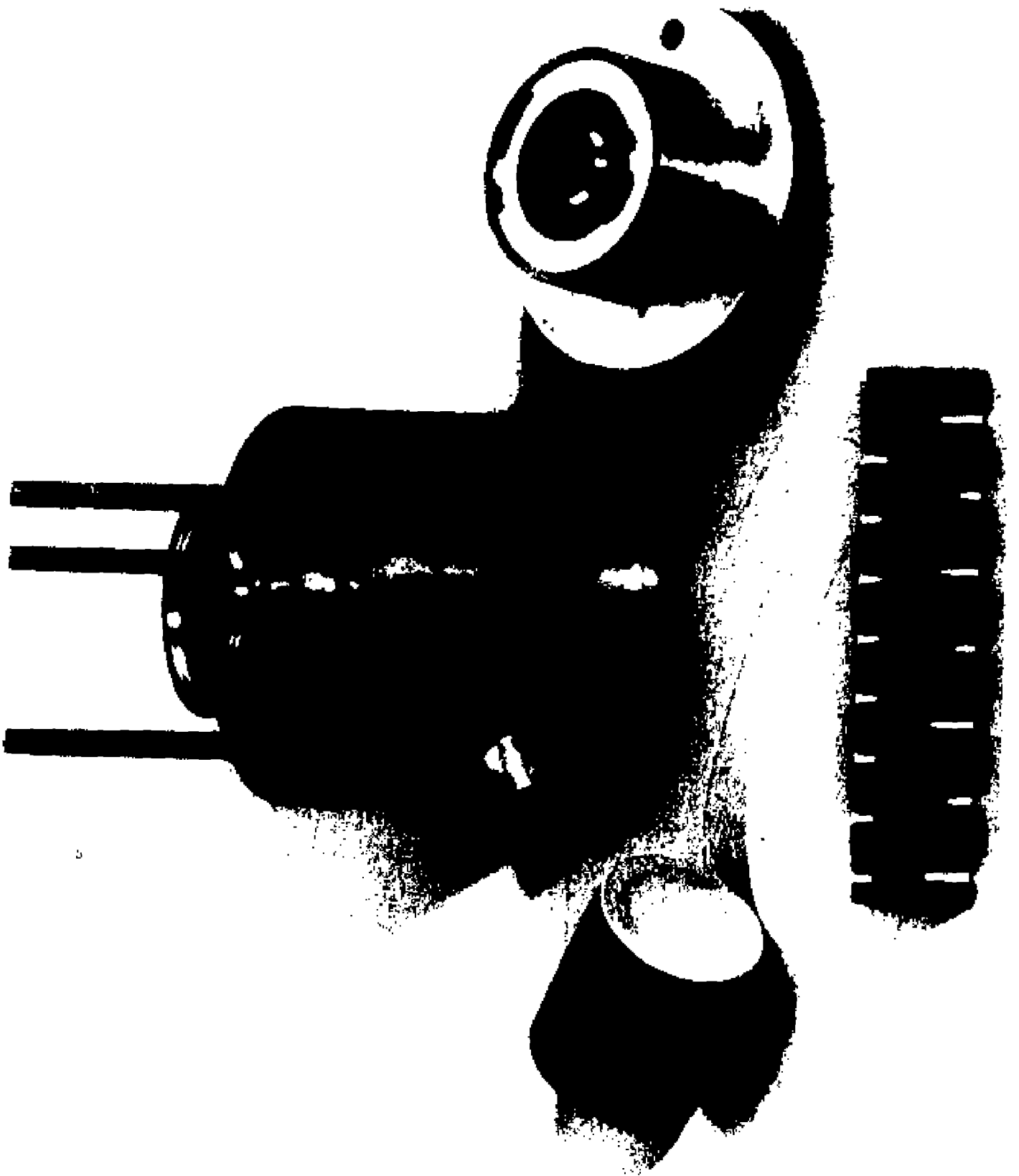
Figure 6. - The dector assembly with the sample
in place.
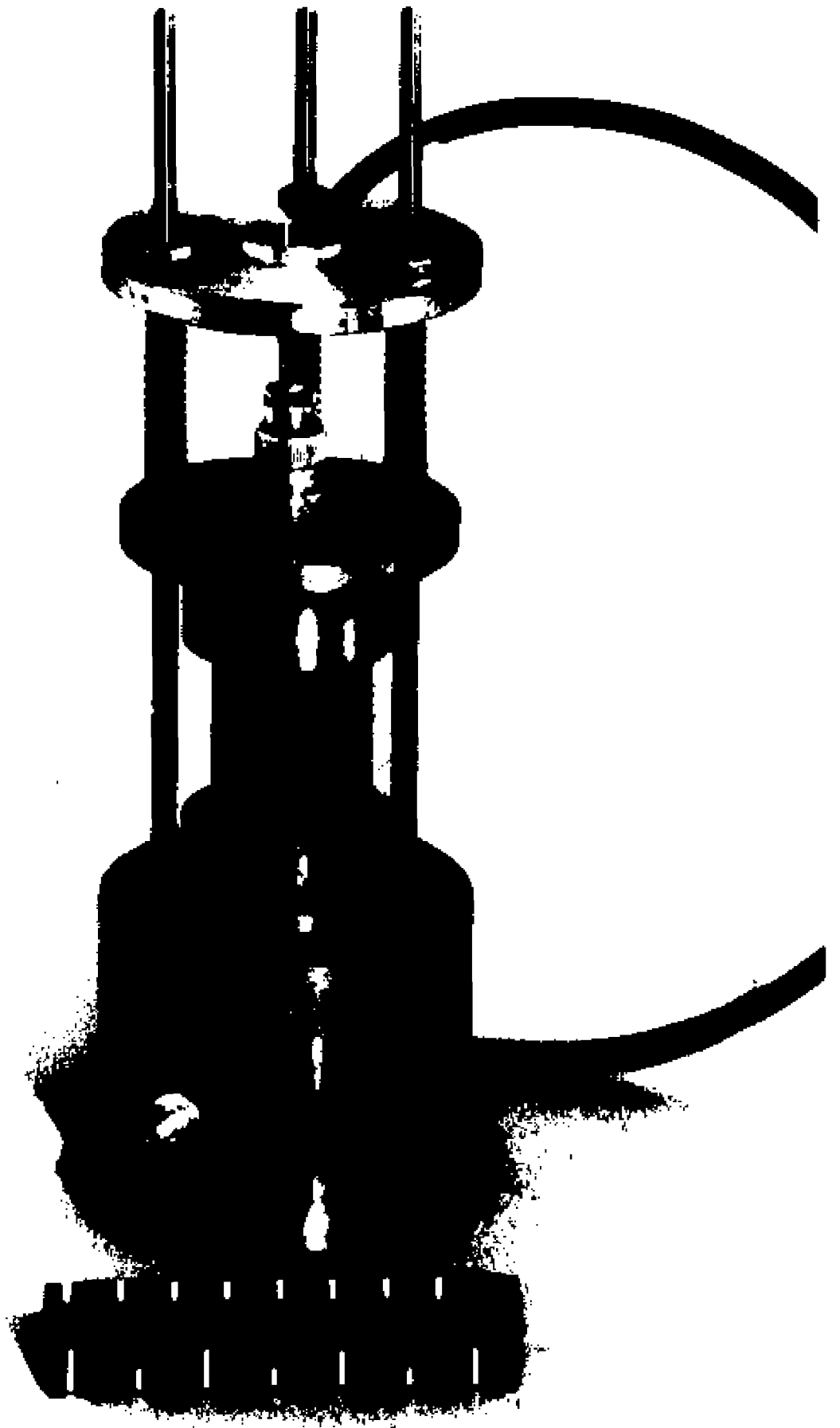
and figure (6) shows the entire system with the sample
in place.

b. Construction of the receiving capacitive transducer.

Since we need to calibrate the system for absolute
displacement measurements, the gap spacing of the parallel
plate capacitor must be determined accurately. It is ,
therefore, necessary to grind and polish the surfaces of
the detecting electrode and samples as flat as possible.
To meet such specifications the signal receiving unit of
the assembly is constructed according to the following
procedure . A thin shim, about seven microns thick, is
placed between the detecting electrode and the glass
plate. The receiving unit is assembled and then lapped
to optical flatness. The flatness of the surfaces are
checked by placing an optical flat on the surface under
consideration and illuminating it with a green light
source to create a Newton's ring pattern. The surface is
considered flat when the fringe density is minimized
and a symmetrical pattern is obtained. Flatnesses
corresponding to one wavelength of green light across
the surfaces are routinely obtained. In the present
experiment no more than one fringe is allowed over the
entire surface of the detecting electrode .

After the surfaces of the receiving unit is lapped to the desire flatness, the shim between the electrode and the glass plate is removed. The unit is reassembled and the position of the electrode is adjusted. The green light source and optical flat are again used to assure that the surfaces are parallel to each other, and that no more than one fringe appears across the entire surface of the electrode.

c. Bonding of the lithium niobate transducer.

The lithium niobate transducer is cemented to the sample by a thin layer of phenyl salicylate according to the following procedure. Both sides of the transducer are cleaned thoroughly with alcohol before bonding. The phenyl salicylate crystals are melted by warming in a clean beaker. After the crystals melt, a small drop is applied to one end of the sample with an eye dropper. The transducer is then placed on top of the liquid so that a thin layer of liquid phenyl salicylate is formed between the transducer and the sample surface. To assure the uniformity of the bond, a slight pressure is applied to the center of the transducer. The bond is then left undisturbed for about an hour. If the surfaces between the bond are clean, the phenyl salicylate will remain in liquid state. To solidify the bond quickly , a small crystal of phenyl salicylate is applied to the

to the edge of the transducer. The whole setup is then left undisturbed for 24 hours.

2. Procedure for measuring the acoustic signals.

From equation (61) we see that in order to determine the value of the nonlinearity parameters, the velocities, the frequency, and the absolute amplitudes of the fundamental acoustic signals, together with the slopes of the static acoustic displacements the frequency of the fundamental signal is monitored by a Hewlett-Packard 5316A universal counter and the velocities of the acoustic waves are obtained from data compiled by Truell, Elbaum, and Chick. [18]

The slopes of the static acoustic displacements and the amplitudes of the fundamental displacements are determined by a substitutional technique in which a Thevenin equivalent network replaces the capacitive transducer and accompying stray capacitance . An appropiate substitutional electrical signal into the network is used to simulate the signal generated at the capacitive transducer by the acoustics. By comparing the response of the appropiate substitutional signals with those of the acoustic signals, the slope of the static acoustic displacement and the amplitude of the fundamental displacement of an acoustic can be

determined. The procedure for calibrating the acoustic signals is given in more detail below.

a. Equivalent circuit for absolute displacement
   measurements.

It is well-established that the Thevenin equivalent circuit of a biased variable gap parallel plate capacitor is that of signal source in series with the quiescent capacitance.[5] The signal source has a voltage magnitude $V = V_b u/s$ where s is the initial gap spacing, V_b the bias voltage, and u the amplitude of the acoustic signal. We shall designate the transducer quiescent capacitance and the accompanying stray capacitance as the Thevenin equivalent network.

The Thevenin equivalent network is shown in figure (7) . The various circuit components in the equivalent network is determined as follows. First the value of the stray capacitance is determined by measuring the capacitance of the assembly before the silicon sample is mounted in place. The system is then assembled so that the surfaces of the silicon sample and the detecting electrode form a parallel plate capacitor . The capacitance is then remeasured . The capacitance of the parallel plate capacitor is obtained by substracting the values of the capacitance before and after the sample is mounted in place .

47

SAMPLE

V_b

1M

1μf

LOW
FREQ

30MHz

C_1

C_2
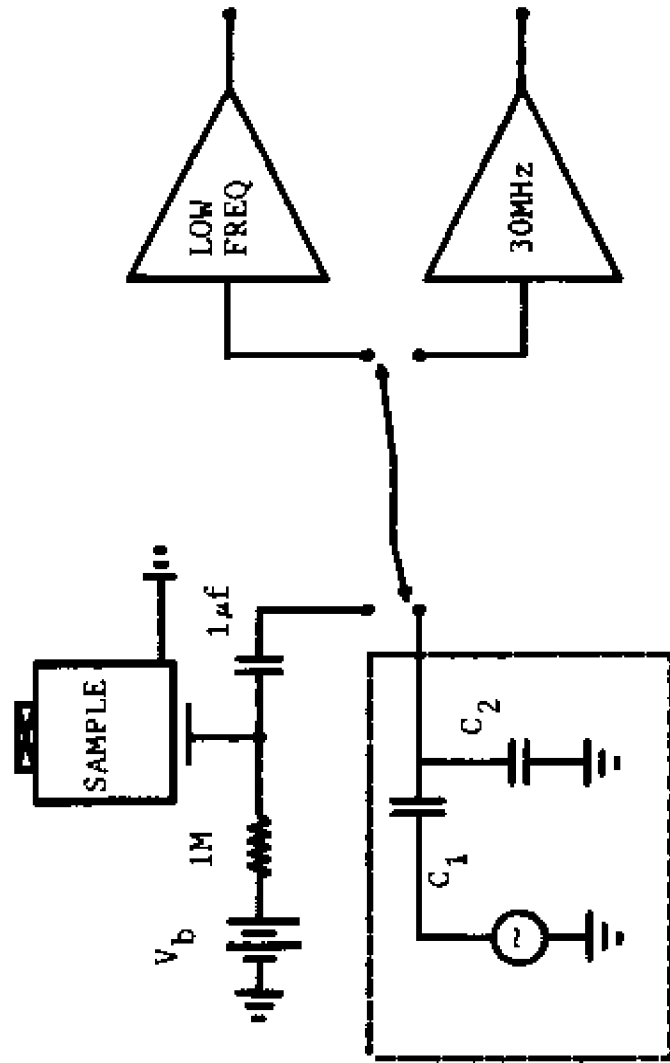
THEVENIN EQUIVALENT NETWORK

figure (7)

The capacitance of the capacitors C_1 and C_2 are adjusted, respectively, to those of the parallel plate capacitor and the stray capacitance.

The gap spacing of the detector is determined by using the relation $s = \epsilon A/C_1$, where A is the area of the parallel plate, and ϵ is the permittivity constant.

After the Thevenin equivalent network is adjusted, we are ready to measure the amplitude of the fundamental acoustic displacement signal and the slope of the static acoustic displacement signal by inputing the appropiate Thevenin sources to the network.

b. Measurement of slope of static acoustic displacement pulse.

A Hewlett-Packard 3314A function generator is used to generate a right-angled trangular substitutional signal having the same width as the acoustic toneburst. This substitutional signal is then sent to the Thevenin equivalent network. The output from the equivalent network is amplified by a Princeton Applied Reasearch 113 preamplifier. The amplified signal is fed to the Biomation/Nicolet unit for signal averaging.

The equivalent network is now switched out and is replaced by the capacitive transducer. Since the preamplifier has a high pass roll off at 300 KHz any

fundamental and higher harmonic signals will be removed after passing through the preamplifier. The amplified static acoustic displacement signal is then sent to the Biomation/Nicolet unit for signal averaging. The amplitude of the fundamental signal is adjusted until the slope of the static displacement signal equals that of the substitutional signal. The slope of the static displacement signal is readily obtained from the substitutional signal.

c. Measurement of toneburst amplitude.

The signal from the capacitive transducer is amplified by an ENI model 3001 RF amplifier. Since the amplitudes of the static acoustic displacement and the higher harmonic signals are approximately one percent of that of the fundamental displacement signal no filtering is necessary before signal amplification. The amplified signal is fed to the sample and hold unit. The sample and hold unit contains a rectifier/filter circuit which rectifies the input signal (see figure (8)), and a sample/hold circuit which holds the voltage at the sampling position. When measurement of the fundamental displacement amplitude is made, the sampling position is adjusted to coincide with the center of the rectified acoustic toneburst. The output from the sample/hold is shown in figure (9). This output is sent to the Hewlett-

Figure 8. – Envelopes of the fundamental signals.

Figure 9. – Output from the sample/hold circuit.
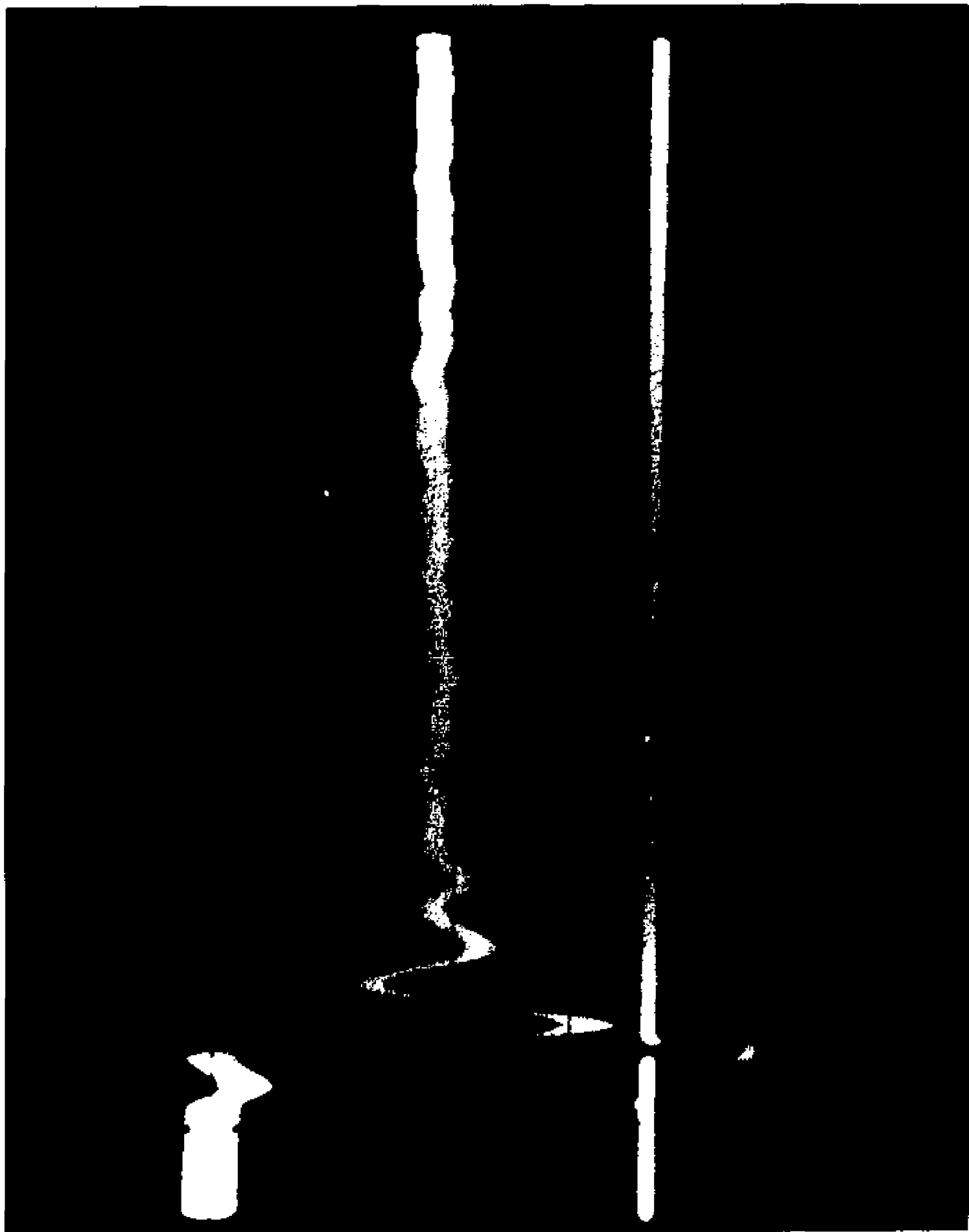
Packard 3478A voltmeter, and its amplitude recorded .

The capacitive transducer is now replaced by the Thevenin equivalent network. A 30 MHz continuous wave substitutional signal is sent to the equivalent network , and its amplitude adjusted until the voltage output from the sample/hold circuit has the same amplitude as that of the acoustic signal. The rms voltage of the substitutional signal is then measured by a Hewlett-Packard 8405A vector voltmeter.

The absolute displacement amplitude of the fundamental signal is determined readily by substituting into the equation [5]

$$u = V \ s/2V_b \qquad\qquad (73)$$

the measured values of V, V_b , and s , where

V = voltage of the acoustic signal,

V_b= the value of the bias voltage,

s = the value of the spacing between the parallel

   plate capacitive detector.

C. samples

Since the amplitude of the acoustic static strains depend on the magnitude of the nonlinearity parameter β_j, an easily grown single crystal with large β_j was sought for the experiments. After a careful literature search for crystals whose nonlinearity parameters had been measured by other techniques,[17,18] we chose silicon.

The cylindrical silicon samples are manufactured by Adolph Muller Co., Providence RI. . They are approximately 1.5 inches long and 1.25 inches in diameter. The propagation (cylindrical) axes of the three samples are oriented along the [111], [110], and [100] directions to within ± 2 degrees. The end faces are perpendicular to the cylindrical axes and are ground and polished to within 0.5 wavelength of visible light. The end faces are parallel to better than 12 second of arc.

D. Determination of the nonlinearity parameters.

According to the present theory the generation of the static acoustic displacement by the fundamental acoustic wave is due to the presence of the nonzero β_j. The nonzero nonlinearity parameters are also responsible for the continuous distortion of an acoustic wave as it propagates through the specimen. Thus, second harmonic generation measurements, for example, can also be used to determine the value of these nonlinearity parameters.

There are, however, advantages of using acoustic static displacement measurements in determining the value of the nonlinearity parameters.

First, from figure (2) we note that the error in determining the amplitude of an acoustic wave due to nonparallelism of the specimen is directly proportional to the inverse wavelength squared. Consequently, error introduced by the second harmonic signal is much larger than that of the static displacement signal. A clear demonstration of this is to use the model given in section A2 and calculate the effect of nonparallelism of the specimen surfaces on the acoustic static displacement pulse. One such calculation is made and the result is given in figure (10). From the figure we note that the leading edge of the pulse becomes distorted, and the width increases as ϕ/λ increases. The slope of the pulse, however, remains essentially constant. The distortion of the leading edge is to some extent a manifestation of the apparent attenuation of the high frequency components of the acoustic pulse, and the increment of its width is due to acoustic path difference between points along the wave front. (e.g. points a and b in figure (2)) .

Second, we note from equation (61) that the acoustic static displacement is directly scaled to the amplitude of the fundamental signal by the nonlinearity parameter.

Effect of nonparallelism of the surfaces of the specimen on the shape of the acoustic static displacement signal.

Displacement

$\epsilon/\lambda =$
0
.01
.05
.1

Normalized length λ

0.0 0.2 0.4 0.6 0.8 1.0 1.2 1.4 1.6
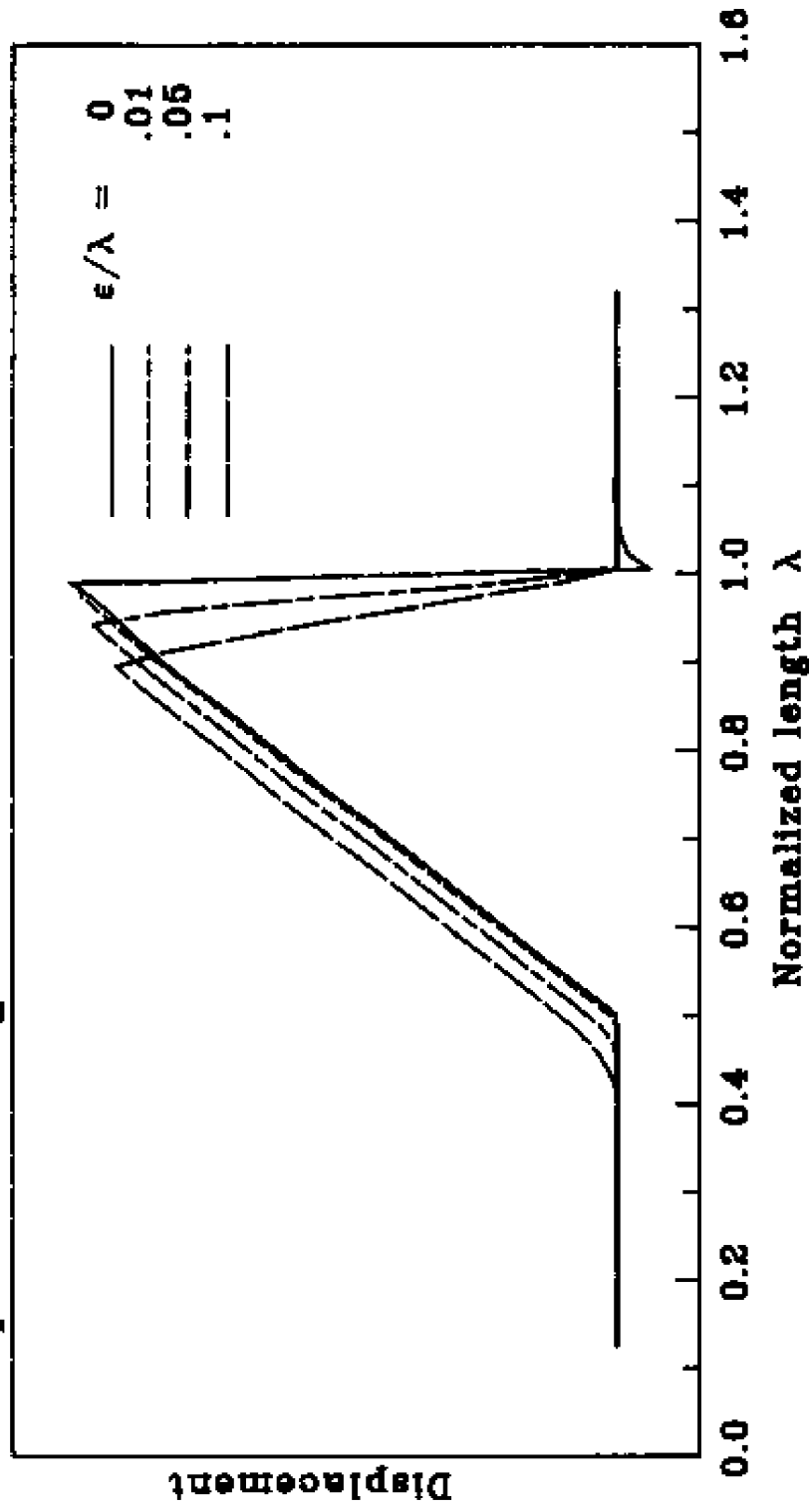
Thus, the sign of the nonlinearity parameter can be determined easily by observing the polarity of the static displacement pulse. In second harmonic generation measurement the sign of the nonlinearity parameter can not be determined without independent measurement of the phase of the fundamental and the phase of the second harmonic signal.[30]

IV. EXPERIMENTAL RESULT

A. Confirmation of the static displacement signal.

The nonlinearity parameters of the single crystal silicon samples along the [111], [110], and [100] directions are determined by measuring the static acoustic displacements generated by a 30 MHz acoustic compressional wave propagating along these pure mode propagation directins at room temperature.

The voltage from the capacitive transducer is equal to $-V_b \frac{2A}{S_0}$, where V_b is the bias voltage, S_0 is the gap spacing of the transducer, and A is the amplitude of the acoustic displacement signal. In the present setup the capacitive transducer is positively biased, hence, an acoustically generated static expansion is expected to produce a negative voltage from the capacitive transducer. And we expect the static acoustic signal to be of the shape shown in figure (11). An oscilloscope trace of the acoustic radiation-induced static displacement signal for an acoustic wave propagating along the [110] direction is given in the bottom of the of figure (12) and the 30 MHz toneburst is displayed at the top of the figure. The
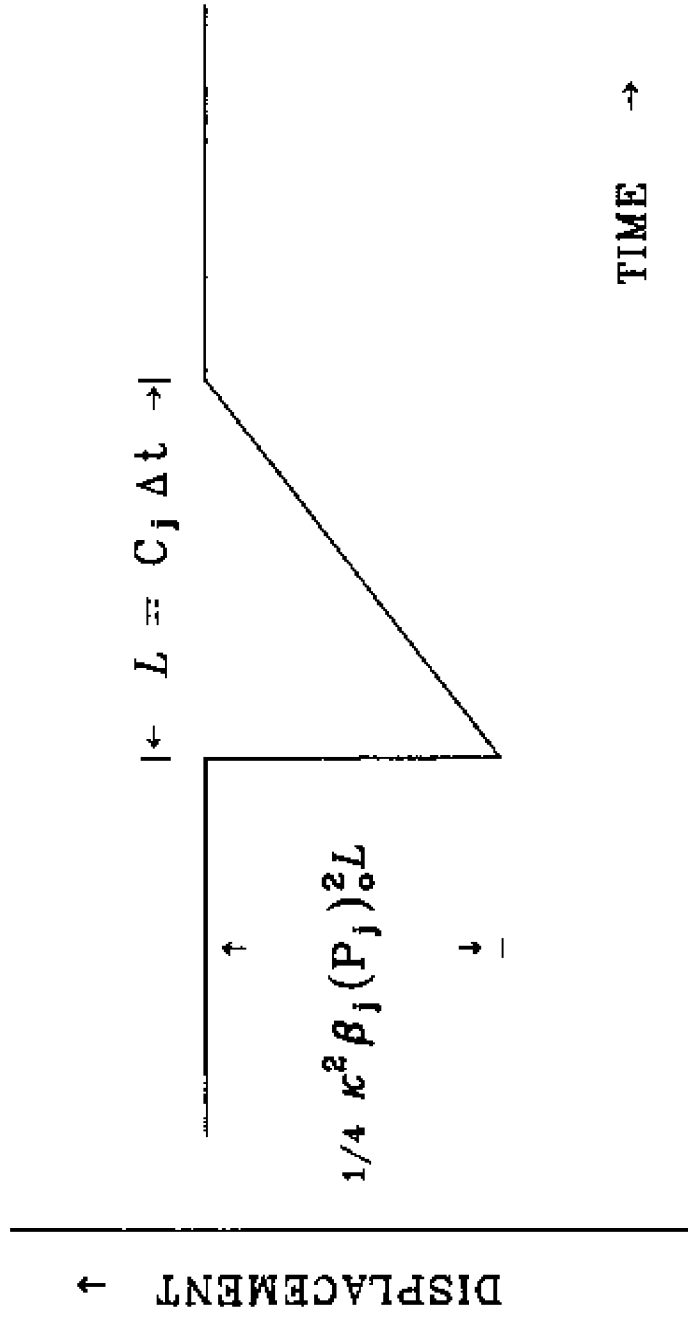
STATIC DISPLACEMENT SIGNAL FROM THE CAPACITIVE DETECTOR.

Figure 12. - Static displacement signal from the

capacitive transducer.

static displacement pulse is negative and is in the shape
of a right angled triangle. Even though the nonparallelism
of the sample surface will introduce some distortion at
the leading edge of the acoustic static displacement
signal, the slow rise time at the leading edge is mostly
due to the bandwitdth limitation of the preamplifier. The
slope of the static acoustic displacement signal, however,
is within the bandwidth of the amplifier. Further, the
substitutional technique used in the measurement assures
that the preamplifier bandpass is not a significant
factor in measuring the slopes of the static acoustic
displacement signals.

An oscilloscope trace of an electronically generated
signal having the shape of a right-angled triangle is
shown at the top of figure (13). The output of the signal
after being sent through the equivalent circuit and the
Princeton Applied Research model 113 preamplier is shown
at the bottom of the figure. The slow rise time in the
leading edge of the signal is clearly shown in the figure.
The slope of the electronically generated signal is used
to calibrate the slope of the acoustic static displacement
signal.

To assure that the observed static displacement
signals are not generated by the electronic circuit, a
simulated 30 MHz tone burst is fed to the equivalent
circuit to check the linearity of the circuit. No static

Figure 13. - Substitutional signal for the acoustic

displacement signal.
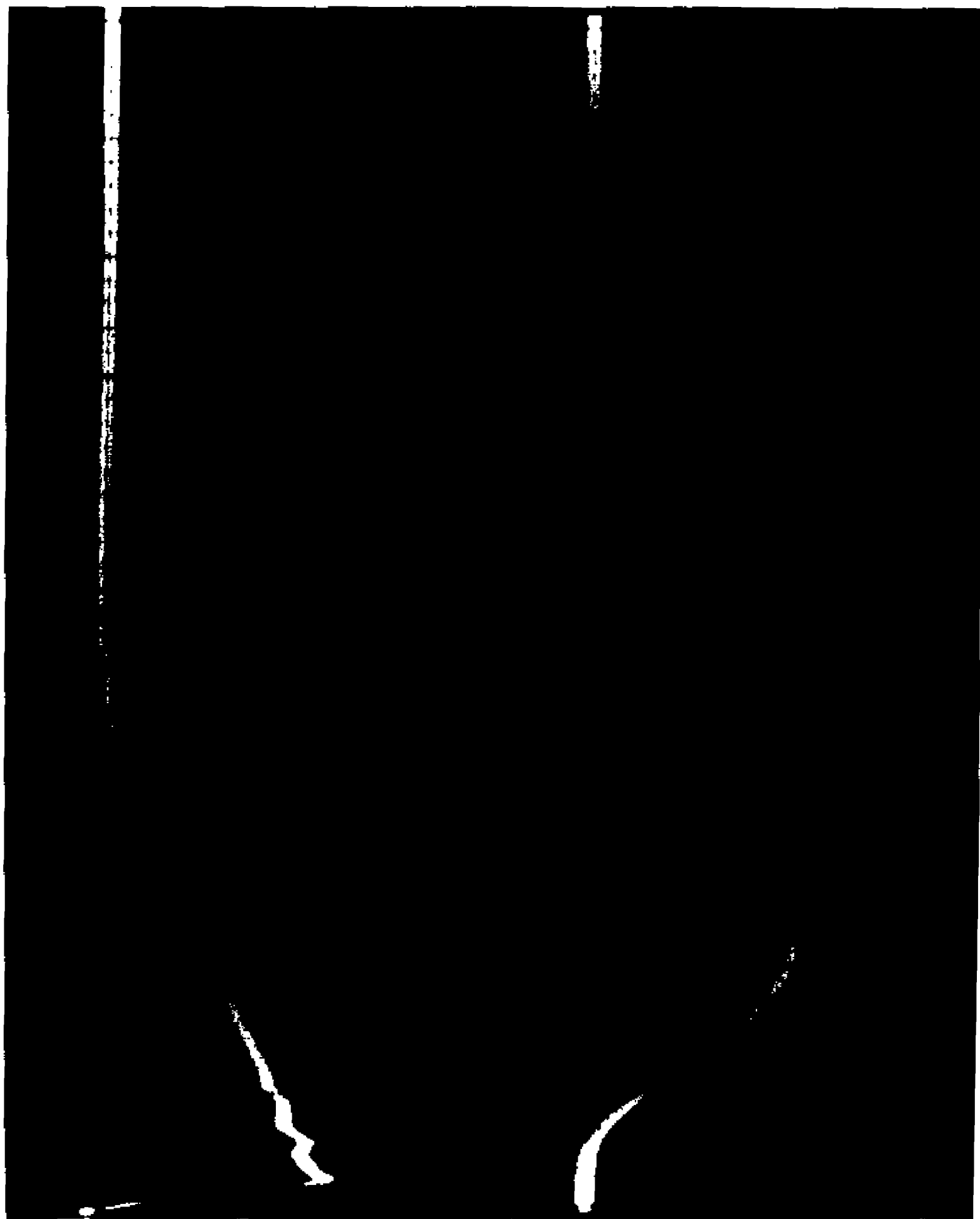
displacement signal is generated even when the amplitude of the simulated signal is above 20 ^{O}A. Since the amplitudes of the fundamental acoustic signals in the present experiment are all less than 20 ^{O}A, the observed static displacement signals are not generated by the electronic circuit.

According to equation (61), the sign of the nonlinearity plays a significant role in the polarity of the acoustic radiation-induced static displacement signal. Fused silica has a negative nonlinearity [31] parameter and is expected to generate a dilative static displacement pulse. This change in polarity with silicon and fused silica has been observed in the present setup and has been reported in the literature. [16]

b. Nonlinearity parameters of silicon single crystals.

According to the present theory, the slope of the static displacement signal is directly proportional to the square of the fundamental displacement amplitude and the square of the propagation number. The velocities of the acoustic waves in the computation of the propagation numbers are obtained from the data compiled by Truell, Elbaum, and Chick. [18]

[111]	[110]	[100]
9.35	9.13	8.43

(in units of cm/sec 10^{-5}). Plots of the square of the static acoustic displacements are shown in figures (14), (15), and (16) for silicon along the pure mode propagation directions. The plots show the linear dependence expected from the theory. Quantitative confirmation of the theory is thus obtained if the nonlinearity parameters calculated from these plots agree with the nonlinearity parameters obtained by other measurements.

In order to calculate the nonlinearity parameters, a least squares fitting of the slopes of the static acoustic displacements versus the product of the fundamental amplitudes are made. The calculated least-square-fit lines are plotted as solid lines in figures (14), (15), and (16). The nonlinearity parameters obtained from these curves are listed in table (2). The nonlinearity parameters based on stress derivative results and those obtained by the second harmonic generation technique are also listed in the table. We see that the nonlinearity parameters obtained from the measurement of the static acoustic displacements are consistent with the nonlinearity parameters obtained from second harmonic generation [17] and stress derivative measurements [18] to within the experimental uncertainty of the measurement techniques.

Figure (14)

SLOPE OF STATIC DISPLACEMENT Vs SQUARE OF FUNDAMENTAL DISPLACEMENT FOR AN ACOUSTIC WAVE PROPAGATING ALONG THE [110] DIRECTION OF A SILICON SINGLE CRYSTAL.

$SLOPE = \frac{1}{8} k^2 \beta_j (P_j)_o^2$

SQUARE OF FUNDAMENTAL DISPLACEMENT (10^{-19} m^2)

SLOPE OF STATIC DISPLACEMENT (10^{-10})
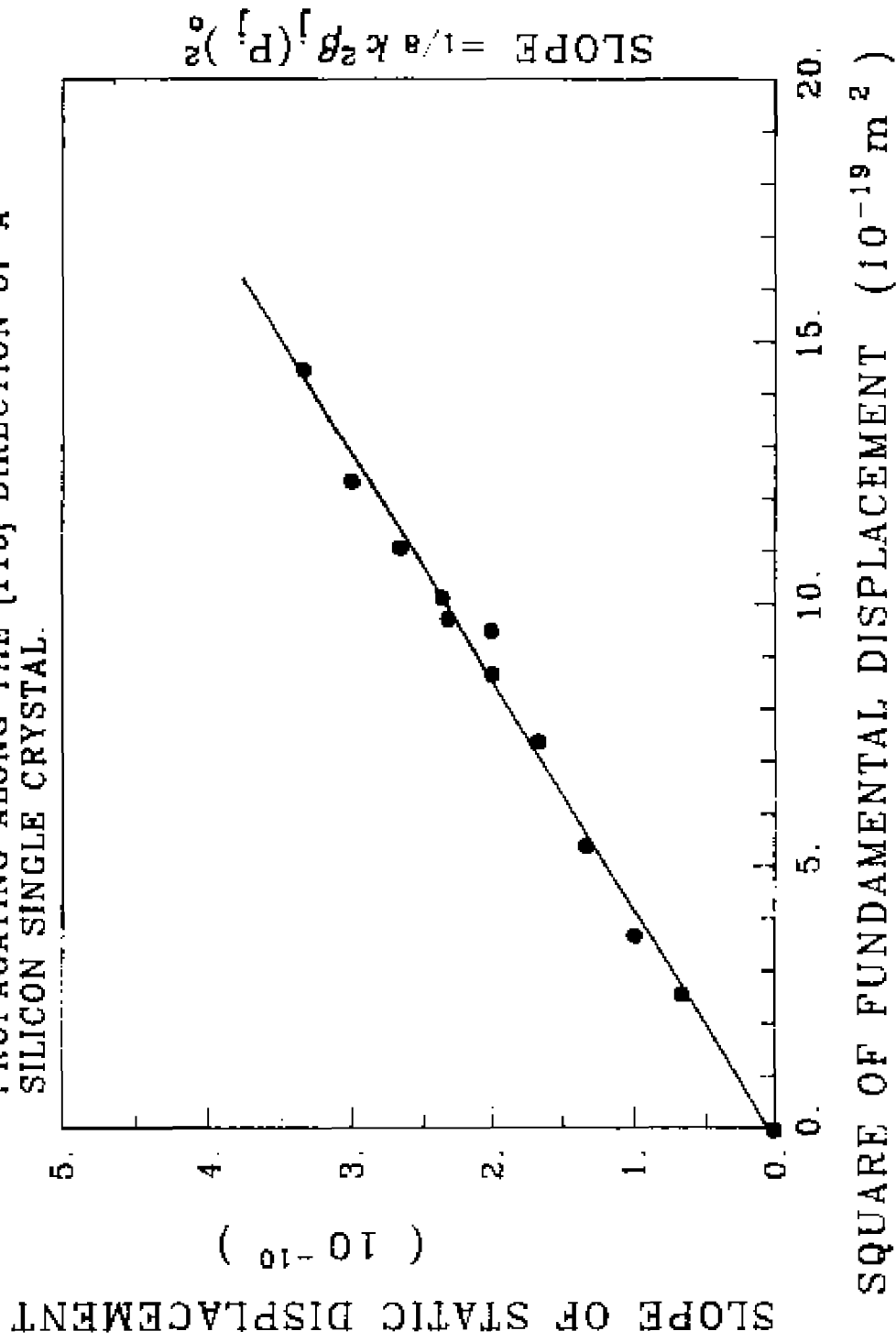
Figure (15)

SLOPE OF STATIC DISPLACEMENT Vs SQUARE OF
FUNDAMENTAL DISPLACEMENT FOR AN ACOUSTIC WAVE
PROPAGATING ALONG THE [111] DIRECTION OF A
SILICON SINGLE CRYSTAL.
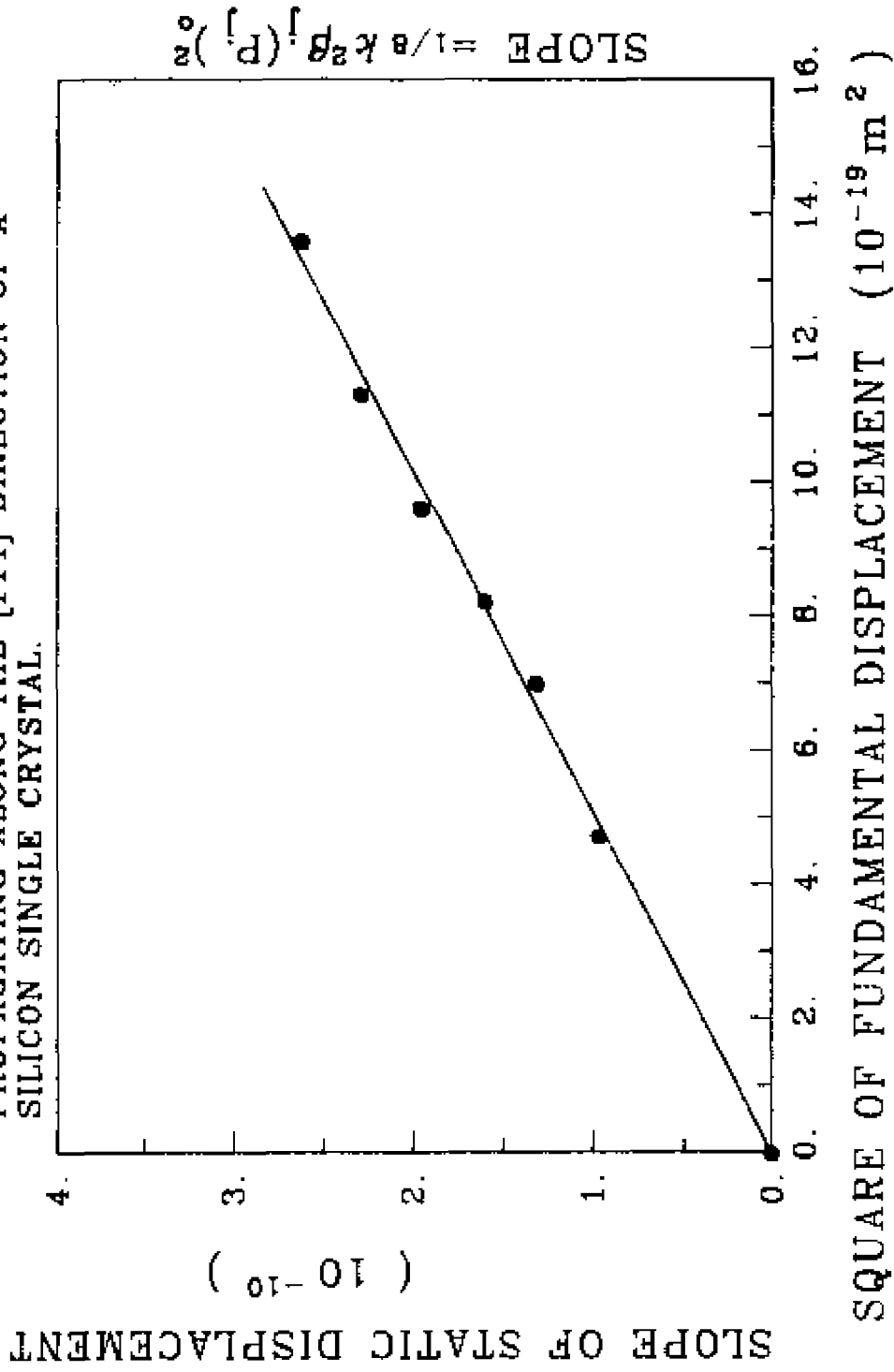
Figure (16)

SLOPE OF STATIC DISPLACEMENT vs SQUARE OF
FUNDAMENTAL DISPLACEMENT FOR AN ACOUSTIC WAVE
PROPAGATING ALONG THE [100] DIRECTION OF A
SILICON SINGLE CRYSTAL.
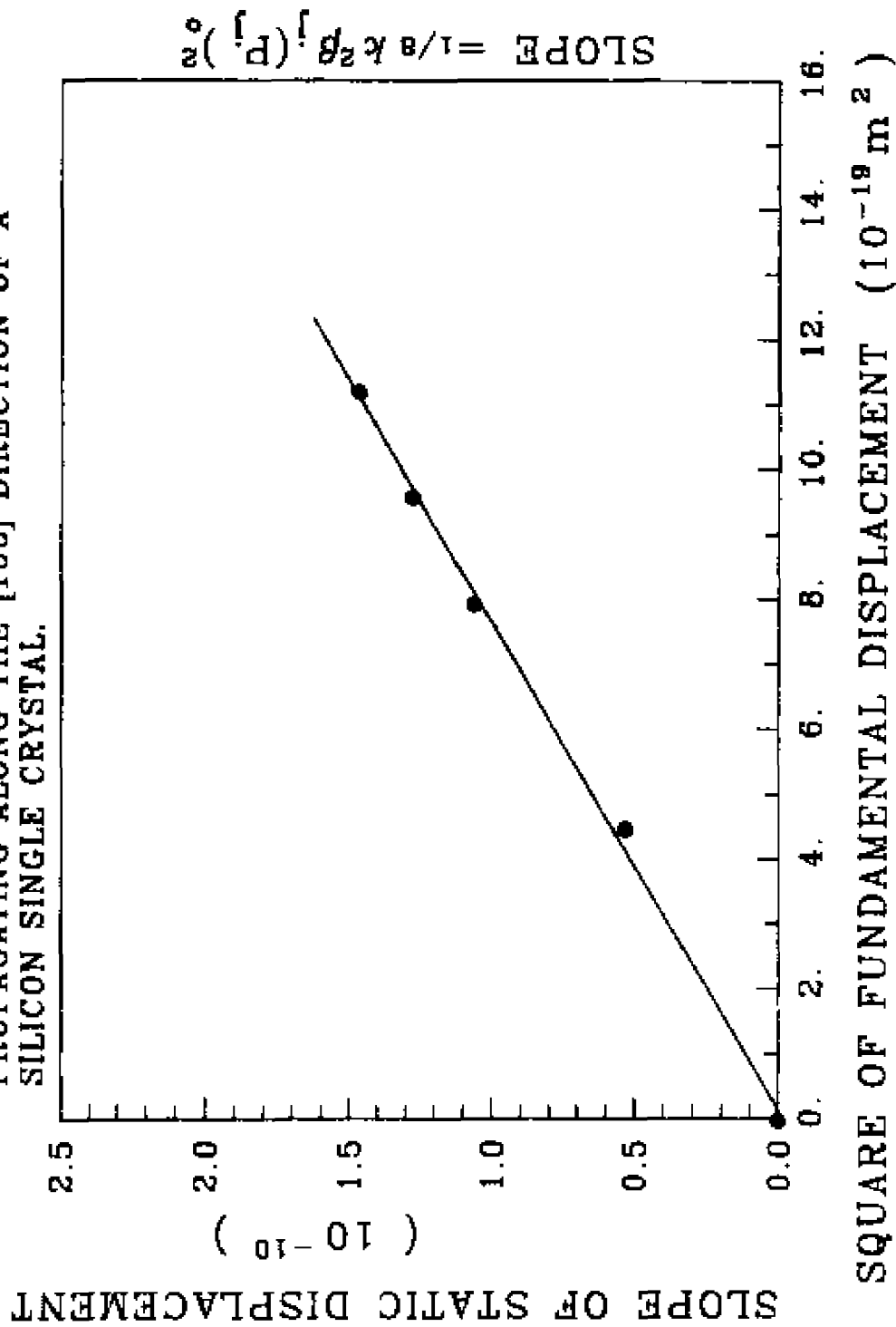
NONLINEARITY PARAMETERS FOR THE [111], [110], AND [100] DIRECTIONS OF SILICON SINGLE CRYSTALS FROM STATIC ACOUSTIC DISPLACEMENT, SECOND HARMONIC GENERATION, AND STRESS DERIVATIVE MEASUREMENTS.

	PRESENT WORK β_j	HARMONIC GENERATION β_j	STRESS DERIVATIVE β_j
[111]	3.87±.58	3.75±.45	3.41±1.61
[110]	4.23±.72	4.69±.56	4.69±.67
[100]	2.13±.36	2.03±.24	1.96±.06

Table 2 .
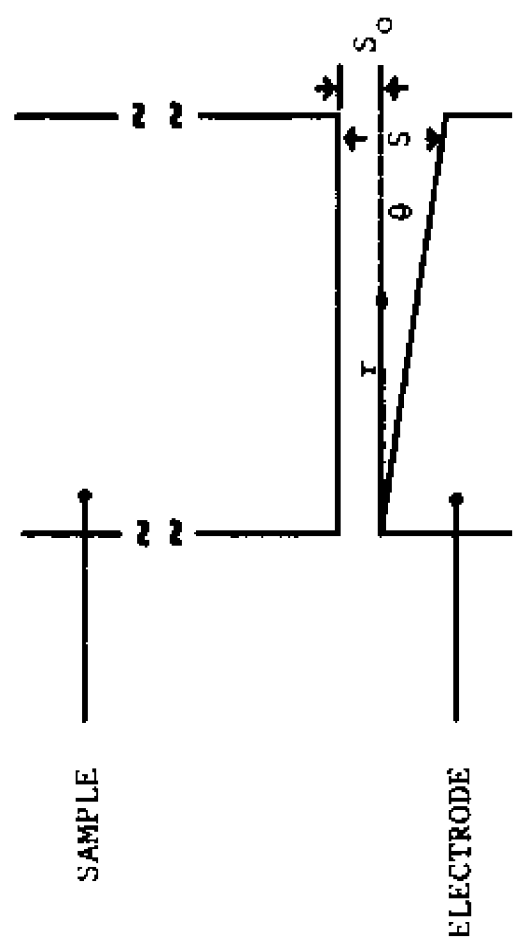
Figure 17.

C. Estimation of the experimental errors.

1. Error introduced by nonparallelisms of the capacitive
   transducer and of the sample surfaces.

Consider the one dimensional model of the capacitive transducer configuration as shown in figure (17). For a small angle θ , the voltage from the capacitive transducer at any instance of time is

$$V = \frac{Q}{C} \qquad , \qquad (74)$$

where

$$C = \frac{1}{L} \int_{o}^{L} \frac{A\ dr}{s_o + r\theta + h} \qquad , \qquad (75)$$

L is the diameter of the transducer, A its surface area, and $h(r,t)$ is the displacement of the sample surface at position r and time t. Since θr and $h(r,t)$ are generally small, equation (74) can further simplified to

$$V = \frac{Q}{\frac{A}{s_o}} \left[1 + \frac{1}{L} \int_{o}^{L} (r\theta + h)\frac{dr}{s_o} \right.$$

$$\frac{1}{L} \int_{o}^{L} (\frac{r\theta}{s_o} + \frac{h}{s_o})^2 dr + (\frac{1}{L} \int_{o}^{L} (r\theta + h)\frac{dr}{s_o})^2$$

$$\left. + \cdots \right] \qquad (76)$$

In the present analysis we wish to estimate the error in measuring the capacitance of the parallel plate capacitor, and the magnitudes of the static and harmonic signals generated due to nonparallelism of the parallel plate capacitive transducer. We, therefore, separate the voltage V into two parts. The voltage which is independent of the acoustic amplitude h, and the voltage V_h which depends on the acoustic amplitude h. Collecting the h independent part to first order, and the h dependent part to second order, we have

$$V = \frac{Q}{C_o} \left(1 + \frac{1}{L} \int_o^L \frac{r\theta}{s_o} \, dr \right) +$$

$$\frac{Q}{C_o} \left[\frac{1}{L} \int_o^L \left(\frac{h}{s_o} - \frac{2r\theta h}{s_o^2} - \frac{h^2}{s_o^2} \right) dr \right] +$$

$$\frac{Q}{C_o} \left[\frac{1}{L} \int_o^L \frac{r\theta}{s_o} \, dr \right] \left[\frac{1}{L} \int_o^L \frac{h}{s_o} \, dr \right] +$$

$$\frac{Q}{C_o} \left(\frac{1}{L} \int_o^L \frac{h}{s_o} \, dr \right)^2 + \dots \quad .$$

When h - 0

$$V = \frac{Q}{s_o} \left(1 + \frac{1}{L} \int_o^L \frac{r\theta}{s_o} \, dr \right) - \frac{Q}{C_o} \left(1 + \frac{L\theta}{2s_o} \right)$$

or

$$V \sim \frac{Q}{C_o (1 - \frac{L\theta}{2s_o})} \tag{78}$$

therefore the first order correction for the capacitive transducer due to nonparallelism of the parallel plates is

$$\left| \frac{\Delta C}{C_o} \right| = \frac{L\theta}{2s_o} \tag{79}$$

In the present experiment $L\theta$ is less than one percent of the wavelength of optical green light. Hence, there is at most a one percent error in estimating the capacitance of the parallel plate capacitor. Since the amplitude of the acoustic signal is inversely proportional to the gap spacing of the parallel plate capacitive transducer, about one percent error is thus introduced in the absolute displacement measurement.

Now let us consider the h dependent part. If we neglect the second order terms in the h dependent part, we have

$$V(t) = \frac{Q}{C_o} [\frac{1}{L} \int_0^L \frac{h}{s_o} dr] \tag{80}$$

Thus, to the first order approximation $V(t)$ is directly proportional to the amplitude of the surface displacement.

In general, however, we see from equation (77) that the voltage from the capacitive transducer also produces static and second harmonic signals. Let us estimate these second order terms for the case where h at any time t is constant along the surface of the sample. This corresponds to the condition whereby the wave front and the specimen surface are parallel to each other. Under this condition $h(r,t) = h(t)$, and

$$V(t) = \frac{Q}{C_o} \left[\frac{h}{s_o} - \frac{L\theta h}{s_o^2} + \frac{h^2}{s_o^2} - \frac{h^2}{s_o^2} + \frac{L\theta h}{s_o^2} \right] + \ldots$$

$$= \frac{Q}{C_o} \frac{h}{s_o} + \ldots \tag{81}$$

Therefore, equation (80) is correct to second order. For the case where h is not constant along the specimen surface, the second order terms, in general, will not vanish. However, the static and harmonic signals from the capacitive transducer are at most of the order

$$\frac{Q}{C_o} \frac{h^2}{s_o^2} \tag{82}$$

Thus, the ratio of the fundamental signal and these second order signals is

$$\sim \frac{h}{s_o} \tag{83}$$

For a typical fundamental dispalcement amplitude of

10 Angstroms and a gap spacing of 10 microns

$$\frac{h}{s_0} \sim 10^{-4}$$

In the present experiment

$$\frac{\text{static displacement}}{\text{fundamental displacement}} \sim 10^{-2}$$

Thus, the second order correction signals can be ignored in the present experiments.

2. Error due to nonlinearity of the capacitive transducer circuit.

A careful analysis of the capacitive transducer circuit by Gauster[5] has shown that the second order signals generated by the capacitive transducer system is of the order h/s_0 . Therefore, the error introduced by this source is of the same order as that introduced by nonparallelism. Both are approximately 40 dB below the acoustic static displacement signal and are ignorable in our measurements.

IV. IMPLICATIONS TO THERMODYNAMICS.

The static strain generated by a finite amplitude
acoustic wave is due entirely to the inherent nonlinear
nature of solids. Acoustic radiation-induced static
strains do not exist for an ideal linear harmonic solid.
Harmonic models are also insufficient to explain many
important thermal properties of solids. For example, in
order to account for the thermal expansion of solids, at
least a quasiharmonic model is needed. [32] In this model,
the solid is considered to consist of a collection of
lattice particles vibrating with small amplitudes about
their equilibrium positions. To account for the presence
of thermal expansion, the distances between the
equilibrium positions of the particles are coupled to
the equilibrium energy of the vibrating particles by the
generalized Grüneisen parameters. If the energy of the
particles increase due to an increase in temperature ,
the distances between the relative positions of the
paritcles increase. Recalling equation (58) we see that
the static displacement of an acoustic wave is also
coupled to the energy of the acoustic wave. It seems
reasonable to suspect, then, that a solid may also be

modeled as a collection of particles vibrating with
finite amplitudes about their initial configureation. In
order to justify our speculation a mathematical
comparison is made between the thermal static strains and
the acoustic static strains.

A. Thermal strains and acoustic nonlinearity.

The thermal static strains of solids can be obtained
by using the quasiharmonic model. In this model a solid
is considered as composed of N particles each vibrating
with a relatively small amplitude about its equilibrium
position. The internal energy of the solid is

$$U = U_o + \sum_{r=1}^{N} (\frac{1}{2} + n_r) \hbar\omega_r \qquad (86)$$

where U_o is the potential energy when all particles are
at rest in their equilibrium positions, and

$$n_r = (e^{\hbar\omega_r/kT} - 1)^{-1} \qquad (87)$$

is the average number of phonons having frequency ω_r at
temperature T .

Using equations (86) and (87), the Helmheltz free
energy is given by

$$F = U_o + \sum_{r=1}^{N} \ln [\ 2 \ \sinh(\hbar\omega_r/kT) \ ] \qquad . \qquad (88)$$

The thermodynamic stress of a solid is given by $\partial F/\partial n_{ij}$. Using equation (88), we can write the thermodynamic stress t_{ij} in the form

$$t_{ij} = \frac{\partial U_o}{\partial n_{ij}} + \frac{\partial F}{\partial n_{ij}} \qquad . \qquad (89)$$

In order to account for the presence of nonlinearity in the quasiharmonic model, U_o and F are expressed as a function of n_{ij} . Taking a Taylor series expansion of the thermodynamic stress in terms of the Lagrangian strains, we obtain to lowest order

$$t_{ij} = \frac{\partial U_o}{\partial n_{ij}} + \frac{\partial^2 U_o}{\partial n_{ij}\partial n_{kl}} n_{kl} - \sum_r \gamma_r^{ij} \epsilon_r \qquad , \qquad (90)$$

where

$$\gamma_r^{ij} = \frac{-1}{\omega_r} \frac{\partial \omega_r}{\partial n_{ij}} \qquad (91)$$

is the generalized Grüneisen parameters, and

$$\epsilon_r = (\ n_r + \frac{1}{2} \ ) \ \hbar\omega_r \qquad (92)$$

is the average energy of the phonons having frequency ω_r.

For the case where all externally applied stresses vanish,

$$t_{ij} = \frac{\partial F}{\partial n_{ij}} = 0 \qquad . \tag{93}$$

If we also assume that no residual mechanical stresses are present

$$\left(\frac{\partial U_o}{\partial n_{ij}}\right)^o = 0 \qquad , \tag{94}$$

and equation (90) becomes

$$c_{ijkl}n_{kl} = \sum_r \gamma_r^{ij}\epsilon_r \qquad . \tag{95}$$

For a cubic crystal we write

$$n_{ij} = n\delta_{ij} \qquad . \tag{96}$$

Subsequently equation (95) becomes

$$c_{ijkl}\delta_{kl}n = \sum_r \gamma_r^{ij}\epsilon_r \tag{97}$$

or

$$n = \frac{\sum_r \gamma_r^{ij} \epsilon_r \delta_{ij}}{c_{ijkl} \delta_{ij} \delta_{kl}} \qquad (98)$$

We shall refer to n in equation (98) as the thermal static strains of solids.

Equation (58) is expressed in terms of the nonlinearity parameters. In order to compare the thermal static strains and the acoustic static strains, we must express equation (98) in terms of the nonlinearity parameters.

The nonlinear wave equation may be written

$$\frac{\partial^2 P_q}{\partial t^2} - c_q^2 \left(1 - \beta_q \frac{\partial P_q}{\partial \bar{a}_1} \right) \frac{\partial^2 P_q}{\partial \bar{a}_1^2} \qquad . \qquad (99)$$

Comparing the nonlinear wave equation with the wave equation

$$\frac{\partial^2 P_q}{\partial t^2} - w_q^2 \frac{\partial^2 P_q}{\partial \bar{a}_1^2} \qquad (100)$$

We readily see that a parametrized " natural wave velocity" for a finite amplitude wave with polarization q and propagation direction $\vec{N}$ may be defined by [10,32]

$$w(q,N) = c_q \left(1 - \beta_q \frac{\partial P_q}{\partial \bar{a}_1} \right)^{\frac{1}{2}} \qquad . \qquad (101)$$

Now in the Debye model the lattic vibrational frequency (q,N) is directly proportional to the natural wave velocity

$$\omega(q,N) \propto w(q,N) \qquad . \qquad (102)$$

Hence, the generalized Grüneisen tensor of equation (91) may be expressed as [10,32]

$$\gamma_r^{ij} = -\frac{1}{\omega_r} \frac{\partial \omega_r}{\partial n_{ij}}$$

$$= -\frac{1}{w} \frac{\partial w}{\partial n_{ij}} \qquad . \qquad (103)$$

In equation (101) the natural wave velocity is parametrized by the factor $\beta_q \partial P_q / \partial \bar{a}_1$. Therefore to evaluate (103) we must make use of the chain-rule differentiation

$$\frac{\partial}{\partial n_{ij}} = \frac{\partial \bar{n}_{pq}}{\partial n_{ij}} \frac{\partial (\partial u_k / \partial \bar{a}_1)}{\partial \bar{n}_{pq}} \frac{\partial (\partial P_q / \partial \bar{a}_1)}{\partial (\partial u_k / \partial \bar{a}_1)} \frac{\partial}{\partial (\partial P_q / \partial \bar{a}_1)} \qquad .$$

$$(104)$$

With the help of the identity

$$\frac{\partial(\partial u_k/\partial \bar{a}_1)}{\partial \bar{n}_{pq}} = \frac{1}{2} (\delta_{kp'}\delta_{1q'} + \delta_{kq'}\delta_{1p'}) \qquad (105)$$

equation (104) can be expressed in the following form,

$$\frac{\partial}{\partial n_{1j}} = \frac{1}{2} S_{kq} (R_{ki}R_{1j} + R_{1i}R_{kj})\frac{\partial}{\partial(\partial P_q/\partial \bar{a}_1)} \qquad (106)$$

Using equation(106) in equation(101), the generalized Gruneisen tensor becomes

$$\gamma_r^{1j} = -\frac{1}{2} S_{kq}(R_{ki}R_{1j} + R_{1i}R_{kj}) \frac{1}{w}\frac{\partial w}{\partial(\partial P_q/\partial \bar{a}_1)} \qquad (107)$$

where

$$-\frac{1}{w}\frac{\partial w}{\partial(\partial P_q/\partial \bar{a}_1)} = \frac{1}{2}\beta_q \qquad (108)$$

Finally the generalized Gruneisen tensor is expressed in terms of the nonlinearity parameters as

$$\gamma_r^{ij} = \frac{1}{4}\beta_q S_{kq}(R_{ki}R_{1j} + R_{1i}R_{kj}) \quad . \qquad (109)$$

Using equation(109) in equation(98), the thermal static

strains may be written as

$$n = \sum_{1,q} \frac{\frac{1}{2} \beta_q S_{kq} R_{kl} R_{1i} \epsilon(q,1)}{C_{mmnn}}$$

(110)

B. Acoustic radiation-induced static strains.

The acoustic static strains are coupled to the energies of the acoustic waves according to the expression

$$\left\langle \frac{\partial P_j}{\partial \bar{a}_1} \right\rangle = 4 \frac{\beta_j}{\mu_j} \left\langle E(1) \right\rangle_j$$

(111)

The acoustic static strains in equation(111) are not referred to the initial Cartesian coordinate frame embedded in the solid but rather to a rotated, diagonalized frame. The thermal static strains on the other hand are referred to the initial reference frame. Therefore, in order to compare the acoustically-induced static strains with the thermal static strains, we must transform equation(111) back into the initial reference frame.

We begin by transforming equation(111) from the diagonalized form into the rotated frame having the a_1-axis along the wave propagation direction

$$\left\langle \frac{\partial \bar{u}_k}{\partial \bar{a}_1} \right\rangle = S_{kj}\left\langle \frac{\partial P_j}{\partial \bar{a}_1} \right\rangle = \frac{1}{4} S_{kj} \frac{\beta_j}{\mu_j} \left\langle E(1) \right\rangle_j \tag{112}$$

Next, we transform equation(112) to the initial Cartesian frame by using the rotational transformation

$$u_{mn} = R_{km} R_{jn} \bar{u}_{kj} \tag{113}$$

in equation(112). We obtain the equation

$$u_{mn} = \frac{R_{km} R_{pn} S_{kj}}{4} \frac{\beta_j}{\mu_j} \left\langle E \right\rangle_j \Gamma_{pl} \tag{114}$$

which gives the displacement gradients in the initial frame. In order to formulate the equation in terms of the Lagrangian strains, we write

$$n_{mn} = \frac{1}{2} (u_{mn} + u_{nm} + u_{rm} u_{rn}) \tag{115}$$

Neglecting the second order terms, the acoustically induced static strains referred to the initial frame become

$$n_{mn} = \frac{R_{km}R_{pn} + R_{kn}R_{pm}}{2} \frac{S_{kj}\beta_j}{4\beta_j} \left\langle E(1) \right\rangle_j \delta_{pl} \tag{116}$$

We now assume that a solid consists of a collection of finite amplitude vibrations which loosely correspond to the phonons of the quasiharmonic model. Summing n_{mn} over all vibrational modes

$$n_{mn}^T = \sum_{j,1} \frac{(R_{km}R_{1n} + R_{kn}R_{1m})}{2} \frac{S_{kj}\beta_j}{4\mu_j} \langle E(1)\rangle_j \qquad (117)$$

From crystal symmetry we expect

$$n_{mn}^T = n_{mn}^T \qquad . \qquad (118)$$

Substituting equation (118) in (117) we obtain

$$n^T = \sum_{j,1} \frac{1}{2} R_{km}R_{1m}S_{kj}\beta_j \frac{\langle E(1)\rangle_j}{2\mu_j} \qquad (119)$$

for the acoustic static strains.

Equation (119) which is obtained by the acoustic static strain model strongly resembles equation (110) obtained from the quasiharmonic model. For ease of comparison we show the results of the two models together

$$n^T_{acoustic} = \sum_{j,l} \frac{1}{2} R_{km} R_{lm} S_{kj} \beta_j \frac{\langle E(1) \rangle_j}{2\mu_j}$$ (120)

$$n_{thermal} = \sum_{j,l} \frac{1}{2} R_{km} R_{lm} S_{kj} \beta_j \frac{\langle E(1) \rangle_j}{C_{uuvv}}$$

where we have identified $\epsilon(j,l)$ with $\langle E(1) \rangle_j$ and replaced q by j in equation (110).

We note a minor difference between the acoustic and thermal static strains. For cubic crystals $C_{uuvv} = 9B$ (where B is the bulk modulus) whereas μ_j in equation (120) is a different combination of second order elastic constants which depends on the direction of propagation of that particular acoustic mode. Nevertheless the strong simularity between the two static strains is obvious.

VI. DISCUSSION

The nonlinearity parameters along the [111], [110], and [100] pure mode propagation directions of silicon single crystals have been determined through measurements of the acoustic radiation-induced static displacements . From these determinations the presence of the acoustic static strains is confirmed.

The existence of these acoustic radiation-induced static strains have interesting implications to other anharmonic properites of solids. For example, we have seen in section IV that the acoustic static strains and the thermal static strains have almost identical mathematical forms. Such simularity suggests that thermal expansion may be understand in the context of acoustic anharmonicity by modeling the solid as a collection of particles vibrating with finite amplitude about their initial configuration . Further investigation of this notion is carried out in appendix 1.

The model given in section IV focused on the nonlinearity parameters of solids. The presence of such nonzero nonlinearity parameters are responsible for the

acoustic harmonic distortion leading to harmonic generation as well as the acoustic static displacement. The nonlinear interaction of a coherent acoustic wave with itself (self-interaction) as well as with an incoherent field of such waves may be of significance to the understanding of nonrelaxational acoustic attenuation. In our present view an acoustic wave suffers nonrelaxational attenuation simply because the medium which supports the wave propagation is nonlinear. Recalling equation (53) , we see that if the medium is viewed as consisting of a set of random acoustic waves plus a coherent acoustic wave propagating through the medium the total signal amplitude may be expressed as

$$A_{total} = \text{acoustic} + \text{random}$$

$$= u(x,t) + f(\text{random})$$

By substituting this expression into the nonlinear wave equation we find that the presence of the nonlinearity parameters will couple the coherent acoustic signal to the random waves existing in the medium. Although we shall not pursue this idea further here (we leave it for future investigation) we expect that the attenuation of the acoustic wave must also be related to the modal Grüneisen parameters of the solid. (The attenuation described here refers only to the loss due to interaction of the acoustic

wave with random waves, and does not include losses due to scattering at the grain boundary , relaxation mechanisms , etc .)

For the most part measurements of nonlinearity parameters, whether by acoustic static strain or second harmonic generation measurements, have been confined to single crystals with a single phase over a wide temperature range. [5-8] A recent investigation [36] shows , however, that the nonlinearity parameters of aluminium polycrystals depend on the degree of mixture with the base metals. In addition, it is well-known that attenuation among the alloys are also strongly dependent on the degree of alloying. Thus if the various contributions to the attenuation of an acoustic wave can be identified, it seems reasonable that such alloy systems may be studied to separate out the relationship between the nonlinearity parameters and the attenuation due to the acoustic-random wave interaction.

Finally, the potential energy of solids are parametrized by the elastic constants when they are modeled as elastic continua. Even when the potential energy of solids are constructed at the atomic level (for example, from the pseudo-potential theory) the accuracy of such models are often tested by how well the second order elastic constants calculated from such atomic

models match the measured elastic constants. However, better insight of the model potentials may be obtained by comparing the calculated and measured higher elastic constants.[33-35]

The third order elastic constants can be computed from the three pure mode nonlinearity parameters for cubic crystals, for example, if three additional independent equations containing the third order elastic constants are given.[4,56,78] The additional equations can be obtained most expediently from stress derivative measurements. The determination of the third order elastic constants through measurements of the nonlinearity parameters are important for solid modeling, whether at the continuum level[17] or at the atomic level.[33]

APPENDIX

Calculation of generalized Grüenisen parameters with the assumption of the presence of static strain.

When a solid is in its equilibrium state, the average net force on any material point in the solid must vanish. Making use of this requirement a relationship between the acoustic radiation-induced static strains and the normal mode acoustic energies for a cubic crystal is formulated. From this relationship an acoustic tensor is defined. The elements of the acoustic tensor along the [111], [110], and [100] pure mode directions are calculated and compared to the generalized Grüneisen tensor defined by other authors.[13,38]

We begin by writing the total stress at any point in the solid as

$$P_{ij} = J_{ik} \frac{\partial \mathcal{E}}{\partial n_{kj}} \tag{A.1}$$

where is the internal energy per unit volume, and

$$J_{ik} = \Gamma_{ik} + \frac{\partial u_i}{\partial a_k} \tag{A.2}$$

We expand $\dfrac{\partial \bar{\Phi}}{\partial n_{kj}}$ in terms of the Lagrangian strains n_{kj} as

$$\frac{\partial \bar{\Phi}}{\partial n_{kj}} = C_{kjmn} n_{mn} + \frac{1}{2} C_{kjmnop} n_{mn} n_{op} + \cdots \quad . \qquad (A.3)$$

Substituting equation (A.3) into equation (A.1) and taking the time and phase averages, we have

$$\langle P_{ik} \rangle = C_{kjmn} \delta_{ik} \langle u_{mn} \rangle + C_{kjmn} \delta_{mn} \langle u_{ik} \rangle +$$

$$\frac{1}{2} C_{kjmn} \delta_{ik} \langle u_{rm} u_{rn} \rangle + \frac{1}{2} C_{kjmnop} \delta_{ik} \langle u_{mn} u_{op} \rangle$$

$$+ O(u^3) \quad , \qquad (A.4)$$

where

$$u_{ij} = \frac{\partial u_i}{\partial a_j} \quad . \qquad (A.5)$$

We assume that the system is composed of a set of random acoustic waves having static and time-dependent components in equilibrium such that the average total stress which is composed of static and time-dependent components must vanish

$$P_{ij} = 0 \quad . \qquad (A.6)$$

Hence, equation (A.4) becomes

$$-C_{ijmn}\langle u_{mn}\rangle = C_{kjmn}\langle u_{mn}u_{ik}\rangle + \frac{1}{2}\langle u_{rm}u_{rn}\rangle C_{ijmn}$$

$$+ \frac{1}{2} C_{ijmnop}\langle u_{mn}u_{op}\rangle \qquad . \qquad (A.7)$$

In order to separate out the static and time dependent components we express the particle displacement in the form

$$u_i = u_i^o + u_i^1 \qquad , \qquad (A.8)$$

where u_i is the total displacement due to the superposition of all possible acoustic modes , u_i^o is the time independent static part of the displacement components and u_i^1 is a superposition of the displacements of a set of random acoustic waves, we write u_i^1 as

$$u_i^1 = U_i(1) \ f_1(N_j(1)x_j(1)-V_j(1)t+\theta_1) + U_i(2)f_2 +\ldots$$
$$(A.9)$$

where

U_i = unit polarization vector,

N_j = unit propagation vector,

θ = random phase.

Hence the time and phase average of equation (A.9) is

$$\langle u_i^1 \rangle = 0 \tag{A.10}$$

Taking the spatial derivative of equation (A.9) we obtain

$$\frac{\partial u_i}{\partial a_j} = U_i(1)N_j(1)f_1' + U_i(2)N_j(2)f_2' + \dots \tag{A.11}$$

where f' denotes the derivative of f with respect to its
argument. Consequently, substituting (A.11) into (A.7),
and using the condition that the cross terms $f_1 f_2$

phase average to zero, we obtain

$$-C_{ijmn}\langle u_{mn} \rangle = [\ C_{kjmn}U_m U_i N_n N_k + \frac{1}{2}C_{ijmn}U_k U_k N_m N_n +$$

$$\frac{1}{2}C_{ijmnop}U_m U_o N_n N_p\ ]_r \langle (f_r')^2 \rangle \tag{A.13}$$

To estimate f_r' we come back to the equation of
motion

$$\rho_o \frac{\partial v_i}{\partial t} = \frac{\partial}{\partial a_j} P_{ij} \tag{A.14}$$

where for convenience we have dropped the index r so that
$v_i = v_i(r)$, $P_{ij} = P_{ij}(r)$ etc. Let us multiply equation

(A.14) by u_i and write

$$\rho_o \frac{d}{dt}(u_i v_i) - \rho_o(\frac{d}{dt}u_i)^2 = \frac{\partial}{\partial a_j}(u_i P_{ij}) - P_{ij}\frac{\partial u_i}{\partial a_j}$$

(A.15)

Since u_i and v_i are bounded we may write

$$\langle \rho_o \frac{d}{dt}(u_i v_i) \rangle = 0$$

(A.16)

Integrating the remaining terms over the volume of the solid we obtain

$$\langle E \rangle = \int_V P_{ij}\frac{\partial u_i}{\partial a_j} dV - \int_S u_i P_{ij} dS_j$$

(A.17)

where we have used the Green's theorm

$$\int_V \frac{\partial}{\partial a_j} u_i P_{ij} dV = \int_S u_i P_{ij} dS_j$$

(A.18)

and have written the modal energy

$$\langle E \rangle = \langle \rho_o(\frac{d}{dt}u_i)^2 \rangle$$

(A.19)

Assuming the surface stress to be zero we write to lowest order in the displacement gradients

$$\left\langle P_{ij}\frac{\partial u_i}{\partial a_j}\right\rangle = C_{ijmn}\left\langle u_{ij}u_{mn}\right\rangle = C_{ijmn}U_iU_mN_jN_n\left\langle (f')^2\right\rangle$$

(A.20)

setting $\mu = C_{ijmn}U_iU_mN_jN_n$ we obtain

$$\int\left\langle (f')^2\right\rangle dV = \frac{\langle E\rangle V}{\mu}$$

(A.21)

Now we can write equation (A.13) in the form

$$C_{ijmn}\int\frac{\langle u_{mn}\rangle}{V}dV = \left\langle\frac{Q^{ij}}{\mu}\right\rangle_r\langle E\rangle_r$$

(A.22)

where

$$-Q_r^{ij} = [\; C_{kjmn}U_mU_iN_nN_k + \frac{1}{2}C_{ijmn}U_kU_kN_mN_n +$$

$$\frac{1}{2}C_{ijmnop}U_mU_oN_nN_p \;]_r$$

(A.23)

To the lowest order approximation,

$$C_{ijmn}\frac{u_{mn}+u_{nm}}{2} = C_{ijmn}n_{mn}$$

(A.24)

If we let

$$\int\frac{n_{mn}}{V}dV = \langle\!\langle n_{mn}\rangle\!\rangle$$

(A.25)

equation (A.22) becomes

$$C_{ijmn} \langle\langle n_{mn} \rangle\rangle - S_r^{ij} \langle E \rangle_r \qquad , \qquad \text{(A.26)}$$

where we have defined the acoustic tensor S_r^{ij} by

$$S_r^{ij} = (\frac{Q^{ij}}{\mu})_r \qquad . \qquad \text{(A.27)}$$

For a cubic crystal

$$\langle\langle n_{mn} \rangle\rangle - n \delta_{mn} \qquad , \qquad \text{(A.28)}$$

therefore equation (A.26) becomes

$$C_{ijmn} \delta_{mn} n = S_r^{ij} \langle E_r \rangle \qquad . \qquad \text{(A.29)}$$

Comparing equation (A.29) with equation (47), we find that the acoustic tensor defined in equation (A.27) must be related to the generalized Grüneisen parameters of solids.

In table (A.1) the acoustic tensor defined in equation (A.27) and the generalized Grüneisen parameters defined by two other authors are given for $ij-11$.

Summary: In obtaining equation (A.29) we assume the presence of a set of random acoustic waves propagating in a continuous medium. The total displacement of a material point is equal to the superposition of the displacements of

the random waves and a static displacement. We find that the static strains are coupled to the energies of the random acoustic waves by an acoustic tensor S_r^{ij}. After comparing equation (A.29) with the thermal static expansion equation, we conclude that the acoustic tensor S_r^{ij} is related to the generalized Gruneisen tensor.

THE GENERALIZED GRUNEISEN PARAMETERS WITH
ij = 11 FOR THE [100], [110], AND [111]
DIRECTIONS OF THE Ge AND Cu SINGLE CRYSTALS.

	$\gamma^{11}(100)$	$\gamma^{11}(110)$	$\gamma^{11}(111)$
PRESENT WORK			
Ge	1.5	1.4	1.1
Cu	2.6	2.7	2.1
CANTRELL			
Ge	1.5	1.5	.9
Cu	2.6	2.8	1.3
BRUGGER			
Ge	1.5	1.5	1.1
Cu	2.6	2.9	2.3

Table A1.

REFERENCES

1. J. G. Collins and G. K. White, Progress in Low temperature physics, vol 4, edited by C. J. Gorter (Wiley, New York, 1964)

2. R. T. Beyer, Nonlinear Acoustic (U.S. GPO, Washingtion, DC, 1975)

3. J.F. Ward and G. H. C. New, Proc. Roy. Soc. $\underline{299}$, 238 (1966)

4. D. C. Wallace, Solid State Physics, Vol 25, edited by H. Ehrenrich, F. Seitz and D. T. Turnbull (Academic Press, New York, 1979)

5. W. B. Gauster, Ph.D. dissertation, The University of Tennessee (ORBL-TM-1573, 1966)

6. R. D. Peter, Ph.D. dissertation, The University of Tennessee (ORNL-TM-2286, 1969)

7. J. H. Cantrell, Jr. and M. A. Breazeale, Phys. Rev. B $\underline{17}$, 4864 (1978)

8. W. T. Yost and M. A. Breazeale, Phys. Rev. B $\underline{9}$, 510 (1974)

9. D. T. Blackstock, J. Acoust. Soc. Am. $\underline{36}$, 534 (1964)

10. J. H. Cantrell, Jr., M.A. Breazeale and Nakamura, J. Acoustic. Soc. Am. $\underline{67}$, 1477 (1980)

11. B. Parrier, J. Phys. (Paris) Colloq 41, C8-216 (1979)

12. J. H. Cantrell, Jr, W. P. Winfree and P. Li, IEEE Ultrasonic Symposium, 2, 1029 (1982)

13. J. H. Cantrell, Jr. To be published in Phys. Rev. Sept (1984)

14. J. H. Cantrell, Jr. and W. P. Winfree, Appl. Phys. lett. 37, 785 (1980)

15. W. T. Yost and J.H. Cantrell, Jr. General Meeting of American Physical Society (1984)

16. W. T. Yost and J. H. Cantrell, Jr. To be published in Phys. Rev. Sept (1984)

17. J. Philip and M. A. Breazeale, J. Appl. Phys. 52, 3383 (1981)

18. R. Truell, C. Elbraum and B. B. Chick, Ultrasonic Methods in Solid State Physics (Academic Press, New York, 1969)

19. J. H. Cantrell, Jr. Journal of Testing and Evaluation 223 (1982)

20. R.N. Thurston, Physical Acoustic, edited by W.P. Mason vol 1A (Academic Press, 1964)

21. F. D. Muraghan, Finite Deformation of an Elastic Solid (Dover Pub. Inc., New York, 1951)

22. K. Brugger, Phys. Rev. 133, A1661 (1964)

23. W. Voigt, Lehrbuch der Kristallphsik (Teubner, Leipzig, und Berlin, 1982)

24. W. T. Yost, Ph.D. dissertation, The University of Tennessee (1972)

25. K. Huang, Proc. Roy. Soc. Lond. A $\underline{203}$, 178 (1950)

26. H. Goldstein, Classical Mechanics (Addison-Wesley, 1981)

27. J. H. Cantrell, Jr. Phys. Rev. B $\underline{21}$, 4191 (1981)

28. A. C. Holt and J. Ford, J. Appl. Phys. $\underline{38}$, 42 (1967)

29. E. Fubini Ghiron, Alta Freq. $\underline{4}$, 530 (1935)

30. A. Bain, Jr. and M.A. Breazeale, J. Acoust. Soc. Am. $\underline{57}$, 745 *1975)

31. J. H. Cantrell, Jr. and M.A. Breazeale, Phys. Rev. B $\underline{17}$, 4864 (1978)

32. K. Brugger, Phys. Rev. A $\underline{133}$, 1604 (1964)

33. K.N. Dhanna and D. P. Khandelwal, Physica B $\underline{111}$, 291 (1980)

34. T. Suzuki, Phys. Rev. B $\underline{3}$, 4007 (1971)

35. T. Suzuki, A. V. Granato and J. F. Thomas, Phys. Rev. B $\underline{175}$, 766 (1968)

36. P. Li, W. P. Winfree, W. T. Yost and J. H. Cantrell, Jr. IEEE Ultrasonic Symposium, $\underline{2}$, 1152 (1983)

37. P. Ehrenfest, Philos, Mag. $\underline{33}$, 500 (1917)

38. W. P. Winfree, J. H. Cantrell, Jr. and P. Li, General Meeting of the American Physical Society (1981)

VITA

<u>Ka Kui Peter Li</u>

Born in Hong Kong, August 11, 1953. He attended the Eastern Oregon State College in La Grande Oregon in 1975, and graduated in June 1979 with a Bachelor of Science degree with a major in Physics. In August 1979 the author enter the College of William and Mary as a graduate assistant in the Department of Physics.